The new spectral Adomian decomposition method and its higher order based iterative schemes for solving highly nonlinear two-point boundary value problems.

by

Madoda Majahonkhe Mdziniso

Dissertation submitted in fulfillment of the requirements of the degree

Master of Science

in

Applied Mathematics

in the

Faculty of Science

at the

University of Johannesburg

Supervisor: Dr M. Khumalo

Co-supervisor: Prof S. S. Motsa

Nov 2013

Abstract

A comparison between the recently developed spectral relaxation method (SRM) and the spectral local linearisation method (SLLM) is done for the first time in this work. Both spectral hybrid methods are employed in finding the solution to the non isothermal mass and heat balance model of a catalytic pellet boundary value problem (BVP) with finite mass and heat transfer resistance, which is a coupled system of singular nonlinear ordinary differential equations (ODEs). The SRM and the SLLM are applied, for the first time, to solve a problem with singularities. The solution by the SRM and the SLLM are validated against the results by `bvp4c`, a well known matlab built-in procedure for solving BVPs. Tables and graphs are used to show the comparison. The SRM and the SLLM are exceptionally accurate with the SLLM being the fastest to converge to the correct solution.

We then construct a new spectral hybrid method which we named the spectral Adomian decomposition method (SADM). The SADM is used concurrently with the standard Adomian decomposition method (ADM) to solve well known models arising in fluid mechanics. These problems are the magneto hydrodynamic (MHD) Jeffery-Hamel flow model and the Darcy-Brinkman-Forchheimer momentum equations. The validity of the results by the SADM and ADM are verified by the exact solution and `bvp4c` solution where applicable. A simple alteration of the SADM is made to improve the performance

of the SADM. The results show that the SADM is more accurate, robust and rapidly converging than the ADM.

We further construct another new spectral hybrid method, namely the reduced quasi-linearisation method (RQLM). We then derive higher order iterative schemes for the RQLM based on the new SADM. The higher order iterative schemes are tested on a class of singular non linear BVPs arising in physiology. Results in literature, exact solution and `bvp4c` results are used to verify the results by the proposed higher order iterative schemes. The study reveals that as we increase the order between two successive higher order iterative schemes the number of iterations reduces by almost half.

Dedication

This work is dedicated to my handsome baby boy, Siyamthanda Khulubuse Mdziniso.

Acknowledgements

My heartfelt gratitude is extended to the following for their input in the success of this work

- My supervisor, Dr M. Khumalo for his tireless support during the course of the study.
- My co-supervisor, Prof S. S. Motsa for his insight and guidance on Spectral hybrid methods.
- The department of mathematics and faculty of science of the University of Johannesburg for giving me the opportunity to pursue my dream by funding this work.
- My family, friends and my soulmate, Noncedo Zulu for inspiring me throughout this journey.
- My Creator, the Lord Almighty for the gift of life and prosperity.

Contents

List of Figures

List of Tables

Chapter 1

Preliminaries

1.1 Introduction

Mathematical modeling is the art of describing a problem or physical system using mathematical concepts and language. The problems vary from simple to sophisticated. Mathematical models are extensively used in the natural sciences, engineering and social sciences. Usually, the mathematical models become very complex, multiple equation systems of ODEs or partial differential equations (PDEs) in the real world. The higher the level of accuracy required the more complex the mathematical model. This is as a result of taking into consideration the system in its entirety without compromising other elements of the problem. The interdependence between the processes within the boundaries of the system and the interaction of the system with the surroundings are also contributing factors to the complexity of the mathematical model. Solutions to sophisticated models are essential for accurate interpretation of the system and precise description of the effects of different components of the problem. They can also be used to give predictions about certain behaviour. Analytical methods are not reliable for solving

such models because they may be too slow to converge to the true solution if convergent at all. Another drawback of analytical methods is the fact that their solution procedures become cumbersome for complex models. For these reasons, numerical methods have become a potential, viable and reliable alternative for solving complicated systems of equations. Extensive numerical and computational skills are required to develop a numerical method that efficiently handles strong nonlinearity, singularities, semi infinite domains amongst other phenomena. Numerical solution procedures have challenges of stability issues and their ability to converge to valid results. The challenges and expectations from numerical methods have provoked the rapid growth in the development of new methods and improvements on existing methods. The ultimate goal is to come up with Numerical Schemes that are more robust, accurate, computationally efficient and easy to implement.

1.2 Spectral hybrid methods

Spectral hybrid methods have recently proven to be more successful than standard methods for complex models. Motsa et al. [1] showed that the spectral homotopy analysis method (SHAM) converges twice as fast as the standard homotopy analysis method (HAM) for the MDH Jeffery-Hamel problem. The successive linearisation method (SLM) developed by Motsa [70] also proved to be highly accurate and rapidly convergent to the exact solution for highly nonlinear problems arising in heat transfer. He further advised that the method performs better than traditional methods like finite differences and the shooting methods. Motsa et al. [3] used the spectral quasi-linearisation method (SQLM) for systems of nonlinear BVPs. The method was found to be computationally efficient and accurate with a rapidly

convergent series solution.

As part of this work, we compare the performance of two newly developed spectral hybrid methods. These numerical techniques are the spectral relaxation method (SRM) and the spectral local linearization method (SLLM). They will be compared for the first time in this work.

1.2.1 The SRM

The SRM was developed by Motsa [4] particularly, for similarity boundary layer problems defined over semi infinite domains in which the governing unknown functions have exponentially decaying profiles. Based on his findings he concluded that the method is not only easy to implement but also highly accurate and computationally efficient. He further advised on the potential of the SRM to be used as a convenient tool to solve a wide class of BVPs. Motsa and Makukula [5] employed the SRM to seek the approximate solution for the von Karman flow of a Reiner-Rivlin fluid with Joule heating, viscous dissipation and suction. The SRM solution was valid and highly accurate for such strongly nonlinear boundary layer type of equations. In their work, they also proposed a novel technique for improving the speed of convergence of the SRM. This approach is based on the very same successive over-relaxation (SOR) used in solving linear systems. Motsa et al. [6] introduced a modification of the SRM namely the multistage spectral relaxation method (MSRM). This extension of the SRM was meant to solve complex dynamical systems of PDEs that exhibit hyper chaotic behaviour. For this problem, the MSRM proved to be accurate and computationally efficient. Motsa and his co-workers [7] applied the MSRM to find the approximate solutions for well known IVPs with chaotic properties. These include Lorenz, Chen, Liu and Rikitake chaotic systems. Similarly, the MSRM was found to

be computationally efficient and accurate. Shateyi and Marewo [8] used the SRM to investigate the MHD flow with heat and mass transfer for the upper-convected Maxwell (UCM) fluid. They transformed the governing PDEs into a system of ODEs prior to applying the SRM. The method continued to yield valid and accurate results.

1.2.2 The SLLM

Motsa [9] introduced the robust, accurate and rapidly converging SLLM approach. The method was tested on strongly nonlinear systems of boundary layer flow problems with exponentially decaying profiles. This method is also used by Motsa and his co-workers [10] to solve a natural convection boundary layer flow problem. The method proved to be an efficient approach for highly non linear BVPs due to its rapid convergence to the solution. It is worth noting that the SRM and SLLM have never been used as a numerical simulation tool for highly non linear BVPs with singularities such as the non-isothermal mass and heat balance model of the porous catalytic pellet BVP with finite mass and heat transfer resistance. This will be done for the first time in this work.

1.3 The Non-Isothermal Mass and Heat Balance Model of the Catalytic Pellet BVP with Finite Mass and Heat Transfer Resistance

Elnashaie and his colleagues [16] derived and solved the model using the Matlab built-in solver for BVPs called `bvp4c` . This model simulates the catalytic reactions at an individual particle level inside a chemical reactor. The growing need for such a study in chemical kinetics was revealed by Kamenetskii [12]. For the past 30 years, there has been an extensive study on how intra-particle diffusion molecules and intrinsic activity influences the overall reaction of porous catalytic pellet [15, 13, 14]. This problem is directly applied in the design of catalytic fixed-bed reactors [16]. Catalytic fixed-bed reactors are the most important type of reactors for the synthesis of large scale valuable chemicals and intermediates in industry, (see [18]). Moreover, fixed-bed reactors have been increasingly used in recent years in the treatment of harmful and toxic substances. For example, the reaction chambers used to remove nitrogen oxides from power station fuel gases constitute the largest type of fixed-bed reactors, in terms of reactor volume and throughput. On the same note, automobile exhaust purification represents by far the most widely employed application of fixed-bed reactors. In these reactors, the reaction takes place in the form of a heterogeneously catalyzed gas reaction on the surface of catalysts that are arranged as a so called fixed bed inside the reactor.

In this work, we also illustrate the development and use of a novel Spectral hybrid technique for solving one dimensional non linear BVPs. We named

this new iterative scheme, the spectral Adomian decomposition method hereinafter referred to as the SADM. The SADM is a blend of the pseudo spectral collocation method by Trefethen [77, 78] and the Adomian decomposition method (ADM). We will further present a slight modification of the SADM which we named the modified spectral Adomian decomposition method (MSADM). The MSADM more than doubles the convergence rate of the SADM.

1.4 The ADM

The semi analytical ADM was developed and presented by G. Adomian in the early 1980s (see [37, 47]). The ADM yields highly accurate analytical approximation to a wider class of nonlinear(and stochastic) equations without linearisation, perturbation theory and discretisation, which can be computationally expensive [37]. Furthermore, this method has excellent accuracy since it is free from round off errors which may arise from discretisation of the solution space [39]. This method has received a lot of attention in the study of various scientific models in biology, physics and applied mathematics due to its efficiency. The ADM is more useful since it can easily and effectively solve linear and highly non-linear functional equations (algebraic, singular and non singular ordinary differential equations, partial differential equations) [40]-[52] and their systems [39, 53, 54], integro-differential equations [55] and delay differential equations [57]. The series solution of this method converged to the exact solution even for stochastic equations without restrictive assumptions on stochasticity [36, 38]. As accurate as the ADM may be there is a room for improvement on the method. Abbasy [47] introduced an Improved ADM(IADM) which is an integration of Pade' approximants and

Laplace transform together with ADM. The method proved to be more effective than the ADM for a special type of non linear PDEs since it increases the region of convergence and hence reveals data that cannot be viewed when using ADM. On another note, Wazwaz [55] presented a reliable modification of ADM that accelerates the convergence of the series solution. Furthermore, Jafari and Gejji [39] introduced a revised ADM that converges faster to the analytical solution for systems of non linear equations than ADM. Most recently, Vahidi and Hasanzade [56] showed that the Restarted ADM(RADM) gives more accurate and suitable solutions for Bratu type problems than ADM in identical conditions. The SADM and ADM will be tested concurrently on two well known problems in fluid mechanics. These are the MHD Jeffery-Hamel Flow and the Darcy-Brinkman- Forchheimer momentum models.

1.4.1 The MDH Jeffery-Hamel Flow problem

The study of the flow of fluids through inclined rigid walls was first conducted by Jeffery [23] and Hamel [24] in 1915 and 1916, respectively. This phenomenon was thereafter called the Jeffery-Hamel flow. This problem is applicable in fluid mechanics as well as aerospace, electrical, mechanical, bio mechanical, civil and environmental engineering [25, 27, 31, 33]. In 1970, Alfven [27] extended the study of the Jeffery-Hamel problem by considering the influence of inducing current in a conductive moving fluid subject to a magnetic field. After introducing the magneto hydrodynamic (MHD) the problem was then called MHD Jeffery-Hamel Flow. The study of magneto hydrodynamic channel has attracted a lot of interest due to its extensive applications in the design of cooling systems with liquid metals, power generators, accelerators, pumps, flow meters and electrostatic meters [25, 27, 33].

Extensive research has been directed at the Jeffery-Hamel flow. Ganji and Azimi [27] showed that the solution obtained when using the differential transformation method (DTM) to the problem is in good agreement with approximate solutions by the Adomian decomposition method (ADM) and the Runge Kutta method of order 4. Bandpay et al [25] used a finite difference method to show that for divergent channel the maximum velocity reduces with increase in the angle between the inclined walls. Moreover, for divergent channels back flow does not occur at any Reynolds number. The Homotopy pertubation method was employed by Nofal [28] to solve divergent and convergent channels and its results compared well with earlier works. Amongst other methods used for this problem is the reduced successive linearisation method (RSLM) by Motsa et al. [22]. This method produced valid results for the solution of the Jeffery Hamel flow when compared with Adomian decomposition method(ADM) and improved Homotopy analysis method. On another note, Imani et al. [29] applied reconstruction of variational iteration method(RVIM) on Jeffery-Hamel flow with high magnetic field and nano particle and showed that the RIVM performed better than perturbation technique and other variational method when considering small parameters and Lagrange multipliers respectively. Ganji et al. [30] showed that both He's variational iteration method (VIM) and He's homotopy perturbation method(HPM) give correct results for MHD Jeffery-Hamel flow when compared with numerical solutions. Alam et al. [31] deduced that the bifurcation points of solution parameters increase due to the effect of Reynolds number using Hermite-Pade' approximations. The Adomian decomposition method yielded more accurate and valid results for MHD Jeffrey-Hamel problem in converging and diverging channel for different angles of the channel, Hartmann numbers and Reynolds numbers when compared with Runge Kutta

method (RK4) [32, 33, 34, 35].

1.4.2 The Darcy-Brinkman-Forchheimer momentum model

The flow of a fluid through a porous medium has also been considered to be of paramount importance over the past 150 years due to its vast applications and implications in physical, biological and applied sciences [59]. Examples of such flow include the flow of ground water, crude oil and gas through the porous earth profiles. There is a host of applications of porous medium flow in irrigation and movement of nutrients, pollutants and gas into plants in agriculture [58] just to mention a few. In this work we shall consider a fully developed pressure driven flow through a fluid saturated porous medium. Such flow is governed by the non linear Darcy-Brinkmann-Forchheimer momentum equations. Motsa et al. [11] showed that the spectral homotopy analysis method is more efficient and converges faster than the standard homotopy analysis method for solving the Darcy-Brinkman-Forchheimer momentum problem. Awartani and Hamdan [59] used second order finite difference schemes to conclude that introducing a porous structure in a flow domain reduces the velocity of the flow. They further reveal that the presence of microscopic inertia also reduces the velocity of the flow. Hooman [60] obtained asymptotic solutions to Darcy-Brinkmann-Forchheimer model for two limiting cases; when $s \gg 1$ and when $s \ll 1$ using a finite difference based scheme. Singh and Thorpe [46] carried out a study to compare the Darcy, Brinkman and Brinkman-Forchheimer models of a free convective flow in an enclosure containing a fluid overlying a porous layer. They employed the false transient method to find solution of each model.

Lastly, we will construct a new generalised reduced quasi-linearisation method (RQLM) and its SADM-based higher order iteration schemes for the

numerical solution of a certain type of singular two point boundary value problems that are essential for the study of tumor growth in biosciences [61, 62]. The RQLM is a hybrid method based on the pseudo Spectral collocation method introduced by Trefethen [77, 78] and the quasi-linearisation method (QLM) of Bellman and Kalaba [63].

1.5 The QLM

Ever since the QLM was developed some 40 years ago, this method has been considered to be powerful due to its rapid quadratic convergence for solving a wide variety of nonlinear ordinary and partial differential equations or their systems. This method has been extensively applied to problems arising in physics, engineering, and biology like orbit determination, radiative transfer, and cardiology [63]. Mandelzweig [64] demonstrated the quadratic convergence of the QLM for more realistic physical problems. He extended the application of QLM to problems with large, infinite domains and singular functions in quantum mechanics. Mandelzweig [65] further established that the QLM converges quadratically when applied to a wider class of non linear BVPs in physics. Ahmad with his co-workers [66] concluded that the QLM converged monotonically and quadratically for Neumann problems. The same conclusion was established by Alsaedi [67] for the duffing equation with mixed boundary conditions. The generalized QLM for second order BVPs with Dirichlet boundary conditions proved to be quadratically convergent [68].

1.6 Overall aims of the study

In this research, we intend to:

- Compare the performance of the SRM against SLLM when solving a coupled system of singular non-linear two-point BVPs.
- Show that the novel spectral Adomian decomposition method performs better than the standard Adomian decomposition method for solving highly nonlinear BVPs.
- Construct the new reduced quasi-linearisation method and its SADM based higher order iterative schemes for solving singular nonlinear BVPs.

1.7 Structure of the dissertation

This dissertation is organized as follows: In Chapter 2, we compare the performance of the SRM against SLLM for solving a coupled system of singular non-linear two-point BVP. Chapter 3 is devoted to the construction of the new SADM and showing that the SADM is superior than the standard ADM for solving highly non-linear two-point BVPs. Chapter 4 covers the development of the new general RQLM and its SADM based higher order iterative schemes for singular non-linear BVPs. The conclusion of the study will be given in detail in Chapter 5. Chapter 6 captures the future development of the study.

Chapter 2

Comparison between the SRM and SLLM on a coupled system of singular highly nonlinear BVPs.

2.1 Introduction

In this chapter, a comparison of the performance between the SRM and SLLM is established. The comparison is based on the level of accuracy, speed of convergence, and stability for each iterative scheme. The convergence speed is measured by the number of iterations taken by each method to converge to the desired level of accuracy. The SRM and SLLM solutions will be compared against `bvp4c` results to see if they are valid. The comparison between SRM and SLLM is presented using tables and graphs. Both methods will be used to treat the non-isothermal mass and heat balance model of the catalytic pellet boundary value problem for the first time.

2.2 Governing equations

We shall consider the case where the external mass and heat transfer resistance is non negligible. Being an exothermic reaction, the heat released can increase the the temperature towards the particle centre [19, 21, 20]. The temperature effect drastically changes the chemical reaction rate which in turn changes the overall behaviour of the catalyst particle in this case. Consequently, the system becomes highly nonlinear. Elnashaie and his colleagues [16] derived the mathematical model describing the mass transfer (x_A) and heat transfer (y) of a porous catalytic pellet reacting inside a tubular chemical reactor in the presence of mass and heat transfer resistance. This phenomenon is governed by a coupled system of singular nonlinear equations with known solutions at the boundaries of the system. This is given as follows:

$$\frac{d^2x_A(\omega)}{d\omega^2} + \frac{2}{\omega}\frac{dx_A(\omega)}{d\omega} - \phi^2 e^{\gamma(1-1/y(\omega))}x_A(\omega) = 0, \tag{2.1}$$

$$\frac{d^2y(\omega)}{d\omega^2} + \frac{2}{\omega}\frac{dy(\omega)}{d\omega} + \beta\phi^2 e^{\gamma(1-1/y(\omega))}x_A(\omega) = 0. \tag{2.2}$$

The solution functions $x_A(\omega)$ and $y(\omega)$ must satisfy the four boundary conditions:

$$\frac{dx_A(0)}{d\omega} = 0, \qquad \frac{dy(0)}{d\omega} = 0, \tag{2.3}$$

$$\frac{dx_A(1)}{d\omega} = Sh[1 - x_A(1)], \qquad \frac{dy(1)}{d\omega} = Nu[1 - y(1)]. \tag{2.4}$$

Here, the functions $x_A(\omega)$ and $y(\omega)$ are mass and heat transfer functions, respectively. Moreover, $\omega \in [0, 1]$ denotes the unit distance travelled by the spherical porous catalyst pellet whilst γ is the dimensionless activation energy and β is the thermicity factor. Furthermore, Sh represents the dimensionless Sherwood number for mass transfer and Nu is the dimensionless

Nusselt number for heat transfer. Sh and Nu are finite since the external mass and heat transfer resistance is considerable.

2.3 Methodology

In this section, we give a general overview of the implementation of the SRM and SLLM iterative schemes for any given non linear coupled system of differential equations.

2.3.1 The SRM

The SRM scheme simply involves rearranging the governing equations in a particular order, starting with the one that has the least number of unknown functions. We then employ the Gauss Seidel technique for purposes of decoupling the system. Usually, the Gauss Seidel is used to decouple linear systems of algebraic equations. Lastly, we linearise the system without using Taylor expansions or any such technique. These three steps break down the nonlinear coupled system into a sequence of linear decoupled subsystems that are easily solved. Below are the steps involved for developing the SRM iterative scheme as given in [5]:

1. Rewrite the equations in some chronological order, starting with the one that has the least number of unknowns. This minimises assumptions.

2. Starting with the first equation, determine the unknown variable with the highest order in each equation. Replace these unknowns with some unique Z_i, $i = 1, 2, 3, \ldots, m$ and m is the total number of non linear equations. This is such that the unknown associated with the highest

order in equations $1, 2, 3, \ldots, m$ is marked as $Z_1, Z_2, Z_3, \ldots, Z_m$, respectively.

3. For the first equation (i.e. $i = 1$), the linear terms in Z_1 are evaluated at the current iteration and hence they are discretised as $Z_{1,r+1}$. The other unknowns $(Z_2, Z_3, \ldots, Z_m)$ appearing in equation 1 are assumed to be computed in the previous iteration and hence they are labeled as $Z_{i,r}$ where $i = 2, 3, \ldots, m$. This facilitates decoupling of the equation. On the same equation, we assume that the nonlinear terms in Z_1 are pre-determined and so they are denoted by r (i.e. $Z_{1,r}$). This serves the purpose of linearizing without the application of Taylor expansion or any other linearizing technique.

4. On the second equation (i.e. $i = 2$), the linear terms in Z_2 are denoted by $r + 1$ since they are evaluated at the current iteration. The recently computed solution of Z_1 in equation 1 is used immediately here and hence each Z_1 must be subscripted as $Z_{1,r+1}$. This is how the scheme resembles the Gause Seidel technique. The other unknowns appearing in equation 2 are assumed to be computed from previous iteration and hence they are labeled as $Z_{i,r}, i = 3, 4, \ldots, m$. We assume that the nonlinear terms in Z_2 are pre-determined and so they are discretised by r (i.e. $Z_{2,r}$). This serves the purpose of linearizing.

5. For $i = 3$, the linear terms in Z_3 are denoted by $r + 1$ since they are evaluated at the current iteration. The recently computed solutions of Z_1 and Z_2 in equations 1 and 2, respectively are used immediately. As a result, Z_1 and Z_2 are denoted by $r + 1$. All the other terms in $Z_3, Z_4, \ldots, Z_m$ are assumed to be pre-determined and hence they are discretised by r.

6. We carry on this process in all the remaining equations. For the last equation, $i = m$, the linear terms in Z_m are discretized as $Z_{m,r+1}$. The nonlinear terms in Z_m are denoted by r. All the other terms(linear or nonlinear) involving $Z_1, Z_2, Z_3, \ldots, Z_{m-1}$ are discretised by $r + 1$ since they are known from the previous equations.

The same iterative scheme is described by Motsa [4] as follows. Consider a system of m non linear ordinary differential equations with m unknown functions $z_i(\omega)$ $(i = 1, 2, \ldots, m)$ where ω is the independent variable in the region [0,1]. We construct the vector Z_i whose elements are all the derivatives of the variable z_i with respect to ω. The vector is given as follows

$$Z_i(\omega) = [z_i^{(0)}, z_i^{(1)}, \ldots, z_i^{(n_i)}],$$

where $z_i^{(0)} = z_i$, $z_i^{(p)}$ is the pth derivative of z_i with respect to ω and $z_i^{(n_i)}(i = 1, 2, \ldots, m)$ is the highest order derivative of the variable z_i in the system of equations.

Each i^{th} equation in the system can be written in the form:

$$\mathcal{L}_i[Z_1, Z_2, \ldots, Z_m] = N_i[Z_1, Z_2, \ldots, Z_m] + H_i(\omega), \quad i = 1, 2, \ldots, m, \tag{2.5}$$

where $\mathcal{L}_i$ and N_i are linear and non linear operators respectively. $H(\omega)$ is a known function in ω.

If we let r and $r + 1$ denote the previous and current iterations then each N_i can be linearised as follows:

$$N_i[Z_1, Z_2, \ldots, Z_m] = N_i[Z_1, Z_2, \ldots, Z_{i,r}, Z_{i+1}, \ldots, Z_{m-1}, Z_m]. \tag{2.6}$$

Applying the Gauss-Seidel approach on the resultant non linear system we develop the SRM iterative scheme as follows:

$$\begin{aligned}
\mathcal{L}_1[Z_{1,r+1}, Z_{2,r}, \ldots, Z_{m-1,r}, Z_{m,r}] &= N_1[Z_{1,r}, Z_{2,r}, \ldots, Z_{m,r}] \\
&\quad +H_1(\omega), \\
\mathcal{L}_2[Z_{1,r+1}, Z_{2,r+1}, Z_{3,r}, \ldots, Z_{m,r}] &= N_2[Z_{1,r+1}, Z_{2,r}, Z_{3,r}, \ldots, Z_{m,r}] \\
&\quad +H_2(\omega), \\
\mathcal{L}_3[Z_{1,r+1}, Z_{2,r+1}, Z_{3,r+1}, Z_{4,r}, \ldots, Z_{m,r}] &= N_3[Z_{1,r+1}, Z_{2,r+1}, Z_{3,r}, \ldots, Z_{m,r}] \\
&\quad +H_3(\omega),
\end{aligned}$$

$\vdots$

$$\begin{aligned}
\mathcal{L}_i[Z_{1,r+1}, Z_{i,r+1}, Z_{i+1,r}, \ldots, Z_{m,r}] &= N_i[Z_{1,r+1}, Z_{2,r+1}, Z_{i-1,r+1}, Z_{i,r}, \ldots, Z_{m,r}] \\
&\quad +H_i(\omega), \qquad (2.7)
\end{aligned}$$

Therefore, starting from the initial approximations $Z_{1,0}, Z_{2,0}, Z_{3,0}, \ldots, Z_{m,0}$ the SRM iterative scheme (2.7) can be repeatedly solved until the desired level of accuracy is reached for all the unknowns$(Z_1, Z_2, \ldots, Z_m)$.

2.3.2 The SLLM

Just like the SRM, the SLLM also imports the Gauss Seidel idea for decoupling the system into a sequence of subsystems. This method then relies on the Taylor series expansion for purposes of locally linearising each subsystem. This gives rise to a new decoupled system of linear equations. A detailed description of how to generate the SLLM iterative scheme is given by Motsa [10]. Below we illustrate the derivation of the SLLM iterative scheme. Let us consider a system of m non linear ordinary differential equations with m unknowns $Z_i(\omega)$ where $i = 1, 2, \ldots, m$ and ω is the dependent variable. For each i^{th} equation, we define linear and nonlinear operators $\mathcal{L}_i[Z_1, Z_2, \ldots, Z_m]$

and $N_i[Z_1, Z_2, \ldots, Z_m]$, respectively as follows

$$\mathcal{L}_i[Z_1, Z_2, \ldots, Z_m] + N_i[Z_1, Z_2, \ldots, Z_m] = H_i(\omega), \quad i = 1, 2, \ldots, m, \tag{2.8}$$

where $H_i(\omega)$ is a known function in ω.

In developing the SLLM iterative scheme we apply local linearisation of N_i for each equation about $Z_{i,r}$. Z_i is discretised as $Z_{i,r+1}$ while $Z_k,\ k \neq i$ becomes $Z_{k,r}$. Here the subscripts r and $r+1$ represent previous and current iterations, respectively. Hence, for each i^{th} equation N_i is given as follows

$$\begin{aligned} N_i[Z_1, Z_2, \ldots, Z_m] &= N_i[Z_{1,r}, Z_{2,r}, \ldots, Z_{m,r}] \\ &\quad + \frac{\partial N_i}{\partial Z_i}[Z_{1,r}, Z_{2,r}, \ldots, Z_{m,r}](Z_{i,r+1} - Z_{i,r}). \end{aligned} \tag{2.9}$$

At each iteration, (2.8) becomes

$$\mathcal{L}_i[Z_1, Z_2, \ldots, Z_m] + \frac{\partial N_i}{\partial Z_i}[\ldots]Z_{i,r+1} = H_i(\omega) + \frac{\partial N_i}{\partial Z_i}[\ldots]Z_{i,r} - N_i[Z_1, Z_2, \ldots, Z_m]. \tag{2.10}$$

where $[\ldots]$ denotes $[Z_{1,r}, Z_{2,r}, \ldots, Z_{m,r}]$. We then employ the Gauss-Seidel approach such that the updated solutions $Z_k, (k < i)$ obtained on previous equations are used immediately for approximating $Z_{i,r+1}$ at the next i^{th} equations. Consequently, the local linearisation iterative scheme can be constructed as follows:

$$\begin{aligned} \mathcal{L}_1[Z_{1,r+1}, Z_{2,r}, \ldots, Z_{m,r}] + \frac{\partial N_1}{\partial Z_1}[\ldots]Z_{1,r+1} &= H_1(\omega) + \frac{\partial N_1}{\partial Z_1}[\ldots]Z_{1,r} \\ &\quad - N_1[Z_{1,r}, Z_{2,r}, \ldots, Z_{m,r}], \\ \mathcal{L}_2[Z_{1,r+1}, Z_{2,r+1}, Z_{3,r}, \ldots, Z_{m,r}] + \frac{\partial N_2}{\partial Z_2}[\ldots]Z_{2,r+1} &= H_2(\omega) + \frac{\partial N_2}{\partial Z_2}[\ldots]Z_{2,r} \\ &\quad - N_2[Z_{1,r+1}, Z_{2,r}, \ldots, Z_{m,r}], \end{aligned}$$

$$\vdots$$

$$\begin{aligned}\mathcal{L}_m[Z_{1,r+1}, Z_{2,r+2}, \ldots, Z_{m,r+1}] + \frac{\partial N_m}{\partial Z_m}[\ldots]Z_{m,r+1} &= \frac{\partial N_m}{\partial Z_m}[\ldots]Z_{m,r} \\ &\quad -N_m[Z_{1,r+1}, Z_{2,r+1}, \ldots, Z_{m,r}] \\ &\quad +H_m(\omega). \qquad (2.11)\end{aligned}$$

here $[\ldots]$ at the i^{th} iteration represents $[Z_{1,r+1}, Z_{2,r+1}, \ldots, Z_{i-1,r+1}, Z_{i,r}, \ldots, Z_{m,r}]$. Therefore, given the initial approximations $Z_{1,0}, Z_{2,0}, Z_{3,0}, \ldots, Z_{m,0}$ the SLLM iterative scheme (2.11) can be repeatedly solved until the desired level of accuracy is reached for all the unknowns$(Z_1, Z_2, \ldots, Z_m)$.

The linear operator $\mathcal{L}$ in the iterative schemes (2.7) and (2.11) can hardly be solved analytically especially when there are more than two linear terms. Consequently, numerical methods such as finite elements, collocation methods, finite differences are used to solve the generated linear iterative schemes. In this work, we shall employ the highly accurate Chebyshev pseudo spectral method. Under this method the approximated linear operators become easily invertible.

To implement this method, it is convenient to first transform the governing physical region [0,1] for the problem to the interval [-1,1] on which the Chebyshev pseudo spectral method is defined. The linear transformation $\omega = (\eta + 1)/2,\ -1 \leq \eta \leq 1$ is used. The solution space [-1,1] is discretised using the Chebyshev-Gauss-Lobatto collocation points

$$\eta_j = \cos\left(\frac{\pi j}{N}\right), \quad j = 0, 1, \ldots N,$$

which are extrema of the N^{th} order Chebyshev polynomial

$$T_N(\eta) = \cos(N \cos^{-1} \eta).$$

N is a non negative integer. We note that there are $N+1$ collocation points. The Chebyshev pseudo spectral method is based on the idea of approximating

the derivatives of the unknown variables $Z_{i,r+1}$ using the Chebyshev spectral differentiation matrix D as a matrix vector product as follows

$$\frac{\mathrm{d}Z_{i,r+1}}{\mathrm{d}\omega} = \sum_{k=0}^{N} \mathbf{D}_{k,j} Z_{i,r+1}(\eta_j) = \mathbf{D}\ \mathbf{Z}_{i,r+1}, \quad j = 0, 1, \ldots, N \tag{2.12}$$

where $\mathbf{D} = 2D$ due to the linear transformation and

$$\mathbf{Z}_{i,r+1} = [Z_{i,r+1}(\eta_0), Z_{i,r+1}(\eta_1), \ldots, Z_{i,r+1}(\eta_N)]^T,$$

is the vector function at the collocation points η_j. In this definition, T means the transpose vector. It follows that

$$Z''_{i,r+1}(\omega) = \mathbf{D}^2 \mathbf{Z}_{i,r+1}.$$

The differentiation matrix D is a square matrix of order $N+1$ whose entries are defined in [77] as

$$\begin{aligned} D_{j,k} &= \frac{c_j(-1)^{j+k}}{c_k\eta_j - \eta_k}, \ j \neq k;\ j,k = 0,1,\ldots,N, \\ D_{k,k} &= \frac{\eta_k}{2(1-\eta_k^2)}, \quad k = 1,2,\ldots,N-1, \\ D_{00} &= \frac{2N^2+1}{6} = -D_{NN}, \end{aligned}$$

where $c_k = \begin{cases} 2 & k=0,N \\ 1 & -1 \leq k \leq N-1 \end{cases}$.

2.4 Applied methods of solution

In this section we briefly outline the application of the SRM and SLLM in solving the system (2.1-2.4).

2.4.1 Solution by SRM

Following the SRM guidelines given earlier on, the linear iterative scheme and boundary conditions for (2.1)-(2.4) are generated as follows:

$$x''_{A_{r+1}} + \frac{2}{\omega}x'_{A_{r+1}} - \Phi^2 e^{\gamma(1-\frac{1}{y_r})}x_{A_{r+1}} = 0 \tag{2.13}$$
$$y''_{r+1} + \frac{2}{\omega}y'_{r+1} = -\beta\Phi^2 e^{\gamma(1-\frac{1}{y_r})}x_{A_{r+1}}$$

subject to

$$x'_{A_{r+1}}(0) = 0, \quad x'_{A_{r+1}}(1) = Sh(1 - x_{A_{r+1}}(1)) \tag{2.14}$$
$$y'_{r+1}(0) = 0, \quad y'_{r+1}(1) = Nu(1 - y_{r+1}(1)) \tag{2.15}$$

Employing the briefly outlined pseudo spectral collocation method to solve the iterative scheme (2.13) we get

$$\mathcal{L}_1 X_{A_{r+1}} = B_1, \tag{2.16}$$
$$\mathcal{L}_2 Y_{r+1} = B_2$$

where

$$\mathcal{L}_1 = \mathbf{D}^2 + a_{1,r}\mathbf{D} - diag(a_{2,r}), \quad \mathcal{L}_2 = \mathbf{D}^2 + a_{1,r}\mathbf{D}, \tag{2.17}$$
$$a_{1,r} = \frac{2}{\omega}, \; a_{2,r} = \Phi^2 e^{\gamma(1-\frac{1}{Y_r})}, \; B_1 = \mathbf{0}, \; B_2 = -\beta a_{2,r} X_{A_{r+1}}. \tag{2.18}$$

From equations (2.18)-(2.18) onwards, $diag()$ means a diagonal matrix of order $(N+1)$, $\mathbf{0}$ is a zero vector of size $(N+1)\times 1$ and the column vectors X_A and Y are the values of the functions x_A and y respectively, when evaluated at the collocation points. We remark that $\mathcal{L}_1$ and $\mathcal{L}_2$ are square matrices of order $(N+1)\times(N+1)$. The Neuman boundary conditions, $x'_{A_{r+1}}(0) = 0$ and $y'_{r+1}(0) = 0$ are imposed on the last row of $\mathcal{L}_1$ and $\mathcal{L}_2$ respectively. The elements of these rows are substituted with corresponding elements of the

last row of $\mathbf{D}$. We then change the last element of B_1 and B_2 to be zero. To implement the boundary conditions at $\omega = 1$, the first row of $\mathcal{L}_1$ and $\mathcal{L}_2$ is replaced with first row of $\mathbf{D}$. On the first element of the first row of $\mathcal{L}_1$ and $\mathcal{L}_2$ we add Sh and Nu respectively. This is such that, $\mathcal{L}_2[1,1] = \mathbf{D}_{1,1} + Sh$ and $\mathcal{L}_2[1,1] = \mathbf{D}_{1,1} + Nu$. The first element of B_1 and B_2 is replaced by Sh and Nu respectively.

2.4.2 Solution by SLLM

According to the SLLM procedure described above, the linear iterative scheme for the system (2.1-2.4) is constructed as follows:

$$x''_{A_{r+1}} + \frac{2}{\omega}x'_{A_{r+1}} - \Phi^2 e^{\gamma(1-\frac{1}{y_r})}x_{A_{r+1}} = 0 \tag{2.19}$$

$$y''_{r+1} + \frac{2}{\omega}y'_{r+1} + \frac{\gamma}{y_r^2}\beta\Phi^2 x_{A_{r+1}} e^{\gamma(1-\frac{1}{y_r})}y_{r+1} = -\beta\Phi^2 e^{\gamma(1-\frac{1}{y_r})}x_{A_{r+1}}(1-\frac{\gamma}{y_r})$$

subject to

$$x'_{A_{r+1}}(0) = 0, \quad x'_{A_{r+1}}(1) = Sh(1 - x_{A_{r+1}}(1)) \tag{2.20}$$

$$y'_{r+1}(0) = 0, \quad y'_{r+1}(1) = Nu(1 - y_{r+1}(1)) \tag{2.21}$$

Employing the briefly outlined Chebyshev pseudo spectral method to solve the iterative scheme (2.19) we get

$$\mathcal{L}_1 X_{A_{r+1}} = B_3, \tag{2.22}$$
$$\mathcal{L}_2 Y_{r+1} = B_4$$

where

$$\mathcal{L}_1 = \mathbf{D}^2 + b_{1,r}\mathbf{D} - diag(b_{2,r}),\ \mathcal{L}_2 = \mathbf{D}^2 + b_{1,r}\mathbf{D} - diag(b_{3,r}), \tag{2.23}$$

$$b_{1,r} = \frac{2}{\omega},\ b_{2,r} = \Phi^2 e^{\gamma(1-\frac{1}{Y_r})},\ b_{3,r} = \frac{\gamma}{Y_r^2}\beta b_{2,r} X_{A_{r+1}}, \tag{2.24}$$

$$B_2 = \mathbf{0},\ B_4 = -\beta X_{A_{r+1}} b_{2,r}(1 - \frac{1}{Y_r}). \tag{2.25}$$

Regardless of the iterative scheme used, the boundary conditions do not change. As a result the boundary conditions here are imposed exactly the same way as we did under Section 2.4.1.

2.5 Test for convergence

To analyse the convergence of the iterative scheme we consider the error due to decoupling (E_d) of the unknown functions for each $(r+1)^{th}$ iteration. E_d is basically the infinity norm of the solutions of each unknown between two successive iterations. That is

$$E_d = Max(\|Z_{1,r+1} - Z_{1,r}\|_\infty, \|Z_{2,r+1} - Z_{2,r}\|_\infty, ..., \|Z_{m,r+1} - Z_{m,r}\|_\infty) \quad (2.26)$$

where $Z_i, i = 1, 2, ..., m$ are the governing unknown functions. Suppose the error due to decoupling at each i^{th} iteration is given by e_i, $i = 1, 2, \ldots, N$ where N is the total number of iteration. Then the iterative scheme is said to be convergent if

$$e_i < e_2 < e_3 < \ldots < e_N. \quad (2.27)$$

This is to say that the iterative scheme is convergent if E_d is inversely proportional to the number of iterations.

2.6 Discussion of results

In this sections we present and discuss the results obtained when solving the the mass and heat balance model of a spherical catalytic pellet using the SRM and SLLM. Figure 2.1 shows a comparison between SRM and `bvp4c` solution profiles of the concentration (x_A) and heat (y) plotted against the unit distance(ω) corresponding to different values of γ. The other governing parameters were fixed at $\beta = 1.1,\ Nu = 10,\ Sh = 250,\ \Phi = \sqrt{1.8}$.

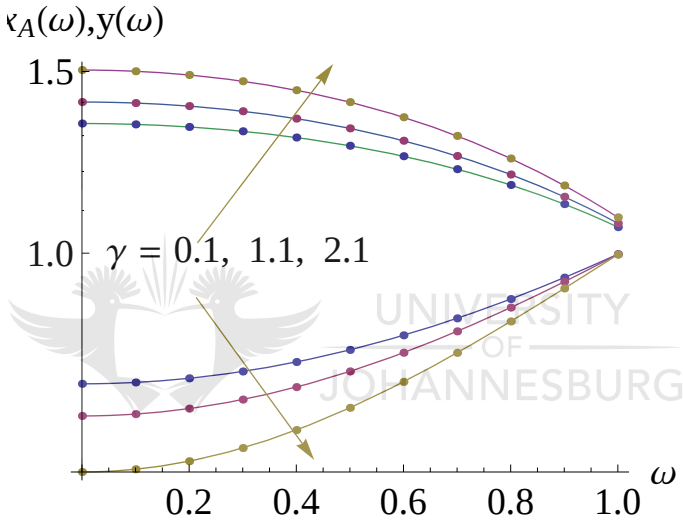

Figure 2.1: Comparison between the SRM(•) and `bvp4c`)(solid line) solutions.

Figure 2.1 shows an excellent agreement between the solution by the SRM and `bvp4c` regardless of the varied values of γ. The figure also shows the relationship between heat and mass transfer. Theoretically, Elnashie and Uhling [16] state that for an exothermic reaction($\beta \approx 1$), the mass xA increases with the decrease in heat transfer y. As a result, there is no doubt that the solution by the SRM is physically correct and valid.

Similarly, Figure 2.2 shows a graphical comparison of the solutions of

$x_A(\omega)$ and $y(\omega)$ between the SLLM and `bvp4c`. Each of the unknown functions was plotted against ω. The values of the governing constants are exactly the same as those used by the SRM to produce the results in Figure 2.1 above.

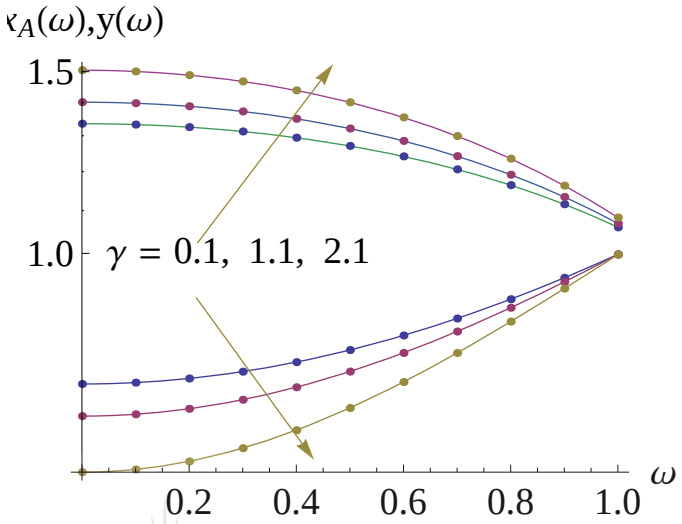

Figure 2.2: Comparison between the SLLM (•) and `bvp4c`)(solid line) solutions.

As we can see from Figure 2.2, the SLLM results are very accurate when compared against `bvp4c` solutions. Furthermore, the solution by the SLLM is very correct when compared with the theory.

The approximate solutions of $x'_A(1)$ and $y'(1)$ by both the SRM and SLLM is exhibited in Table 2.1 and Table 2.2 respectively. A comparison is made with the `bvp4c` results for each solution. The governing parameters Sh and Nu are varied while the others remain constant with $\omega = 1.1,\ \beta = 1.1,\ \Phi = \sqrt{1.8}$.

Table 2.1: Comparison between the SRM and SLLM against `bvp4c` approximate solution for $x'_A(1)$ with different values of Sh and Nu.

$N = 20,\ \beta = 1.1,\ \gamma = 1.1,\ \Phi = \sqrt{1.8}$				
sh	Nu	**SRM**	**SLLM**	`bvp4c`
100	10	0.624166720709827	0.624166720709827	0.624166720709824
100	20	0.607644936269405	0.607644936269405	0.607644936269402
100	30	0.602169811539029	0.602169811539029	0.602169811539026
200	10	0.626403755139296	0.626403755139296	0.626403755139294
200	20	0.609721117147644	0.609721117147644	0.609721117147641
200	30	0.604193826416474	0.604193826416474	0.604193826416471
300	10	0.627153391696794	0.627153391696794	0.627153391696792
300	20	0.610416637398030	0.610416637398030	0.610416637398027
300	30	0.604871800952481	0.604871800952481	0.604871800952479
400	10	0.627528956953204	0.627528956953204	0.627528956953202
400	20	0.610765050174513	0.610765050174513	0.610765050174510
400	30	0.605211411161793	0.605211411161793	0.605211411161790

Table 2.2: Comparison between SRM and SLLM against `bvp4c` approximate solution of $y'(1)$ for varying values of Sh and Nu.

$N = 20,\ \beta = 1.1,\ \gamma = 1.1,\ \Phi = \sqrt{1.8}$				
sh	Nu	**SRM**	**SLLM**	`bvp4c`
100	10	-0.686583392780809	-0.686583392780809	-0.686583392780806
100	20	-0.668409429896346	-0.668409429896346	-0.668409429896342
100	30	-0.662386792692932	-0.662386792692932	-0.662386792692928
200	10	-0.689044130653226	-0.689044130653226	-0.689044130653223
200	20	-0.670693228862408	-0.670693228862408	-0.670693228862405
200	30	-0.664613209058122	-0.664613209058122	-0.664613209058118
300	10	-0.689868730866474	-0.689868730866474	-0.689868730866471
300	20	-0.671458301137833	-0.671458301137833	-0.671458301137829
300	30	-0.665358981047729	-0.665358981047729	-0.665358981047726
400	10	-0.690281852648525	-0.690281852648525	-0.690281852648522
400	20	-0.671841555191964	-0.671841555191964	-0.671841555191961
400	30	-0.665732552277972	-0.665732552277972	-0.665732552277969

From Table 2.1, the SRM and SLLM converge to the same correct solution of $x'_A(1)$ for each different pair of Sh and Nu. The methods converge to 13 digits accuracy when compared against the matlab built-in solver for BVPs. Looking at Table 2.2, the same can be said about the very methods for the approximate solutions of $y'(1)$. Table 2.3 shows the number of iterations taken by the SRM and SLLM iterative schemes to converge to the approximate initial solution of the unknown functions $x_A(\omega)$ and $y(\omega)$. Both methods we set to use only 20 collocation points and values of the governing parameters were fixed as shown in the table.

Table 2.3: Comparison between the SRM and SLLM against `bvp4c` approximate solution for $x_A(0)$ and $y(0)$

.

$N = 20,\ \beta = 1.1,\ \gamma = 1.1,\ Nu = 10,\ Sh = 250,\ \Phi = \sqrt{1.8}$				
iter	**SRM**		**SLLM**	
	$x_A(0)$	$y(0)$	$x_A(0)$	$y(0)$
2	0.719363458058448	1.371045690067426	0.679308872579155	1.396661281603140
4	0.695915056134818	1.400613126435892	0.695448718530627	1.401177406084555
6	0.695474047218013	1.401172797764229	0.695465449213677	1.401183680691276
8	0.695465635985487	1.401183480798991	0.695465471879534	1.401183689192725
10	0.695465475050529	1.401183685215553	0.695465471910241	1.401183689204242
12	0.695465471970386	1.401183689127916	0.695465471910283	1.401183689204258
13	0.695465471918598	1.401183689193696	0.695465471910283	1.401183689204258
14	0.695465471911433	1.401183689202797	0.695465471910283	1.401183689204258
16	0.695465471910305	1.401183689204230	0.695465471910283	1.401183689204258
18	0.695465471910283	1.401183689204258	0.695465471910283	1.401183689204258
20	0.695465471910283	1.401183689204258	0.695465471910283	1.401183689204258
`bvp4c`	$x_A(0)$	$y(0)$		
	0.695465471910284	1.401183689204257		

From Table 2.3, the SRM took 18 iterations to converge to the correct solutions of $x_A(0)$ and $y(0)$ with an absolute error of 10^{-14}. The SLLM on the other hand took 6 iterations lesser to reach the same level of accuracy. This makes the SLLM to be quite faster than the SRM. Both the SRM and SLLM solutions are valid when compared with the `bvp4c` solutions.

Figure 2.3 shows the number of iterations plotted against the error due to decoupling in logarithmic scale by the SRM and SLLM. The tolerance level was set to be $\ln(E_d) \leq 10^{-12}$ during the computation by each iterative schemes. The governing parameters used are $\omega = 1.1,\ \beta = 1.1,\ Nu = 10,\ Sh = 250,\ \Phi = \sqrt{1.8}$.

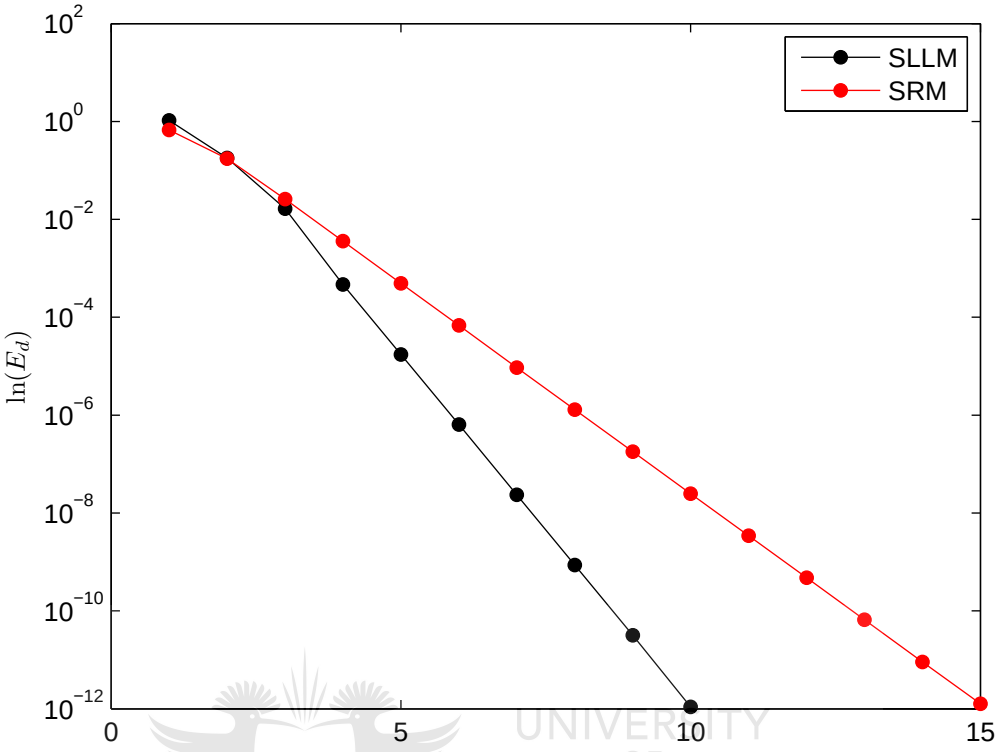

Figure 2.3: Logarithm of the Error due to decoupling($\ln(E_d)$) by the SRM and SLLM against iterations.

From Figure 2.3, we observe that both the SRM and SLLM converge linearly to the approximate solution. Another point worth noting is the fact that the SLLM took only 15 iterations whilst the SLLM took 5 more iterations to reach the tolerance level. This suggest that the SLLM is faster than the SRM for this problem. This can also be seen by the slopes of the graphs.

Similarly, Figure 2.4 shows the number of iterations plotted against the error due to decoupling in logarithmic scale by the SRM and SLLM. The stopping criterion used during the computations was 20 iterations for each it-

erative scheme. The governing parameters used are $\omega = 1.1,\ \beta = 1.1,\ Nu = 10,\ Sh = 250,\ \Phi = \sqrt{1.8}$.

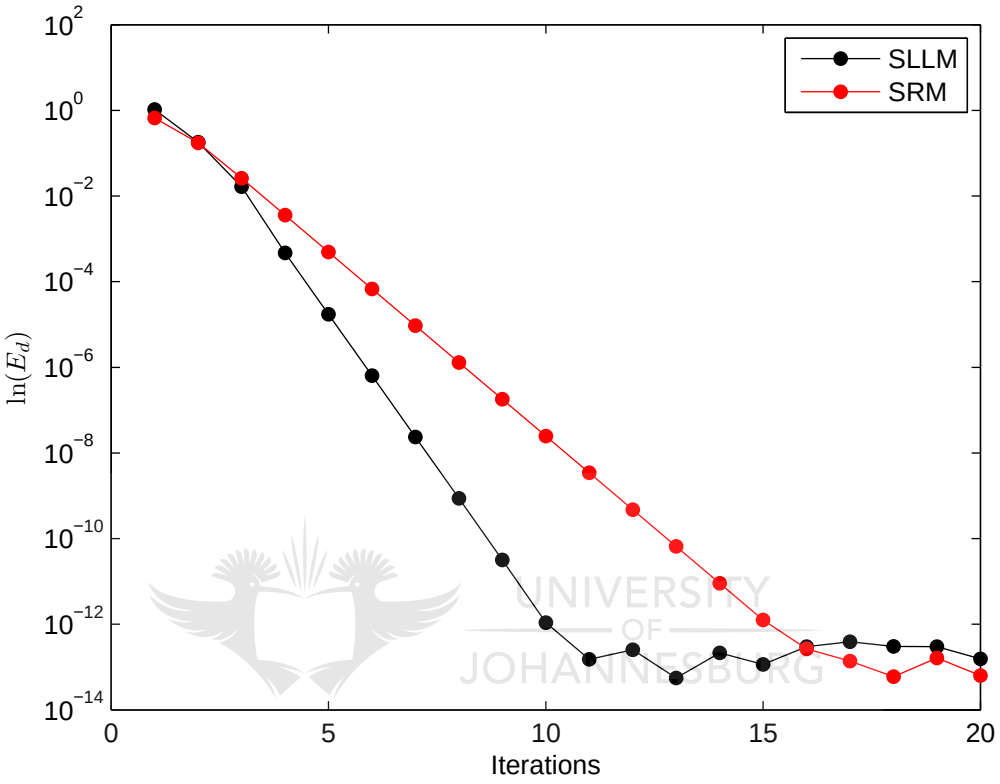

Figure 2.4: Logarithm of the Error due to decoupling($\ln(E_d)$) by the SRM and SLLM against iterations.

In Figure 2.4, we can see that for both methods, there exist a maximum number of iterations such that further increase in the number of iterations results in some inconsistency with the decrease of E_d as they converge to the approximate solution. The zigzag behaviour of the graphs by SLLM and SRM beyond 10 and 15 iterations, respectively is evidence of a small unpredictability of E_d beyond a certain number of iterations for each method.

Chapter 3

The novel SADM for solving nonlinear two-point BVPs

In this chapter we present a novel spectral hybrid method called the spectral Adomian Decomposition Method, abbreviated SADM, as a reliable alternative method for solving nonlinear two-point BVPs. This method is developed by blending the well known Adomian decomposition method (ADM) with the pseudo Spectral collocation method. We further present a simple modification of the SADM called Modified Spectral Adomian Decomposition method (MSADM) which doubles the convergence rate of the SADM. The ADM, SADM and MSADM are used concurrently to obtain solutions for the MDH Jeffery-Hamel flow problem and Darcy-Brinkman-Forchheimer momentum equations arising in Fluid Mechanics. The approximate numerical solutions to the models are compared against exact solutions and `bvp4c` results where applicable. A comparison between ADM, SADM and MSADM is done to show that the SADM and MSADM performs better than the standard ADM.

3.1 Mathematical formulation of the problems

In this section we begin by showing the mathematical formulation of the MHD Jeffery-Hamel phenomena and the derivation of its exact solution. We then present the mathematical model of the Darcy-Brinkman-Forchheimer problem.

3.1.1 MHD Jeffery Hamel problem

The derivation of the MHD Jeffery-Hamel problem is done in [1, 30, 84] as follows. Consider the steady two dimensional flow of an incompressible conducting viscous fluid from a sink or source at the vertex of two rigid plane walls making a channel. The angle between the two plates is 2α as shown in Figure 3.1.

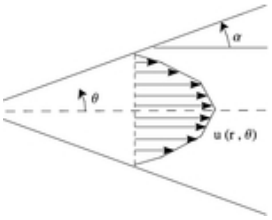

Figure 3.1: Geometry of Jeffery-Hamel flow in a divergent channel

The rigid walls are considered to be divergent if $\alpha > 0$ and convergent if $\alpha < 0$. We assume that the motion is purely radial which means that there is no flow parameter in the z-direction. The velocity depends on r and θ so that $\mathbf{v} = (u(r, \theta))$ only. The continuity equation and Navier-Stokes equations

in polar coordinates are given by:

$$\frac{\rho}{r}\frac{\partial}{\partial r}(ru(r,\theta)) = 0, \tag{3.1}$$

$$u(r\theta)\frac{\partial u(r,\theta)}{\partial r} = -\frac{1}{\rho}\frac{\partial P}{\partial r} + v\left[\nabla^2 u(r,\theta) - \frac{u(r,\theta)}{r^2}\right] - \frac{\sigma \mathbf{B}_0^2}{\rho r^2}u(r,\theta), \tag{3.2}$$

$$0 = -\frac{1}{\rho r}\frac{\partial P}{\partial \theta} + \frac{2v}{r^2}\frac{\partial u(r,\theta)}{\partial \theta}. \tag{3.3}$$

Introducing P as the fluid pressure, $\mathbf{B}_0$ the electromagnetic induction, σ the conductivity of the fluid, ρ the fluid density and v is the coefficient of kinematic viscosity. From continuity equation (3.1)

$$u(r,\theta) = \frac{f(\theta)}{r}. \tag{3.4}$$

We define the following dimensionless parameters

$$y(x) = \frac{f(\theta)}{U_{max}}, x = \frac{\theta}{\alpha}. \tag{3.5}$$

Substituting (3.5) into (3.2)-(3.3) and eliminating the pressure term yields the following non linear third order differential equation

$$y(x)''' + 2\alpha Re y(x)y'(x) + (4 - H)\alpha^2 y'(x) = 0 \tag{3.6}$$

subject to the following boundary conditions

$$y(0) = 1, \quad y'(0) = 0, \quad y(1) = 0. \tag{3.7}$$

Here, $Re = \frac{\alpha U_{max}}{v}$ is the Reynolds number and $H^2 = \frac{\sigma \mathbf{B}_0^2}{\rho v}$ is the square of the Hartmann number.

The above boundary conditions are as a result of the fact that $\frac{\partial u(r,\theta)}{\partial \theta} = 0$ at the centreline of the channel and $u(r,\theta) = 0$ at the plates making the body of the channel. It is worth mentioning that for convergent channels $U_{max} < 0$ and that $U_{max} > 0$ in the case of divergent channels.

3.1.2 The analytical solution of the governing Jeffery-Hamel equation

Recently, Abbasbandy and Shivanian [84] have introduced a way of finding the exact solution of the system (3.6)-(3.7) as follows. Integrating the governing equation (3.6) we get

$$y(x)'' + 2\alpha Rey(x)^2 + (4-H)\alpha^2 y(x) = A, \tag{3.8}$$

where A is the constant of integration. Taking the transformation $w = \frac{\mathrm{d}y}{\mathrm{d}x}$, we have

$$y''(x) = w\frac{\mathrm{d}w}{\mathrm{d}y}. \tag{3.9}$$

Substituting equation (3.9) into (3.8) and then integrate we get

$$\frac{1}{2}y'^2(x) + \frac{1}{3}\alpha Rey^3(x) + \frac{1}{2}(4-H)\alpha^2 y^2(x) = Ay(x) + B, \tag{3.10}$$

where B is another constant of integration.

Employing the first and second boundary conditions on equations (3.8) and (3.10) we get

$$\begin{aligned} A &= \gamma + \alpha Re + (4-H)\alpha^2, \\ B &= \frac{1}{3}\alpha Re + \frac{1}{2}(4-H)\alpha^2 - A \\ &= -\frac{2}{3}\alpha Re - \frac{1}{2}(4-H)\alpha^2 - \gamma, \end{aligned} \tag{3.11}$$

assuming that $\gamma = y''(0)$. Rewriting equation (3.10) we get

$$\left(\frac{\mathrm{d}y}{\mathrm{d}x}\right)^2 = 2Ay + 2B - \frac{2}{3}\alpha Rey^3 - (4-H)\alpha^2 y^2. \tag{3.12}$$

Substituting the integration constants (3.11) in (3.12) and then integrate yields

$$x = \int_1^y \frac{\mathrm{d}\tau}{\sqrt{2(g_0\tau - \frac{2\alpha Re}{3} - \frac{(4-H)\alpha^2}{2} - \gamma) - \frac{2\alpha Re\tau^3}{3} - (4-H)\alpha^2\tau^2}} \tag{3.13}$$

where

$$g_0(\gamma;\alpha,H,Re)=\gamma+\alpha Re+(4-H)\alpha^2.$$

If we set

$$G(y,\gamma;\alpha,H,Re)=\int_1^y \frac{\mathrm{d}\tau}{\sqrt{2(g_0\tau-\frac{2\alpha Re}{3}-\frac{(4-H)\alpha^2}{2}-\gamma)-\frac{2\alpha Re\tau^3}{3}-(4-H)\alpha^2\tau^2}}, \tag{3.14}$$

then

$$G(y,\gamma;\frac{-\pi}{36},0,60)=\frac{-\left(\frac{3i\sqrt{5}}{5}\sqrt{g_1-\sqrt{g_2}}\sqrt{g_1+\sqrt{g_2}}EllipticF\left(\frac{g_3}{\sqrt{g_4-\sqrt{g2}}},\frac{\sqrt{g_4+\sqrt{g_2}}}{\sqrt{g_4-\sqrt{g_2}}}\right)\right)}{\pi^{\frac{1}{4}}\sqrt{g_4-\sqrt{g_2}}\sqrt{g_5}}, \tag{3.15}$$

where

$$\begin{aligned}
g_1(y) &= 720\sqrt{\pi}y-\pi^{\frac{3}{2}}+360\sqrt{\pi},\\
g_2(\gamma) &= \pi^3-2160\pi^2+1166400\pi-933120\gamma,\\
g_3(y) &= 12i\sqrt{5}\pi^{\frac{1}{4}}\sqrt{y-1},\\
g_4 &= 1080\sqrt{\pi}-\pi^{\frac{3}{2}},\\
g_5(y,\gamma) &= 360\pi y^2-\pi^2y+360\pi y+648\gamma-720\pi+\pi^2.
\end{aligned}$$

Therefore, the exact analytical solution of the MHD Jeffery-Hamel flow system (3.6)-(3.7) in an implicit form is given by

$$x=G(y,\gamma;\alpha,H,Re). \tag{3.16}$$

The unknown parameter γ referred to as the skin friction can easily be obtained by substituting the third boundary condition of equation (3.7) into (3.16) as follows

$$1=G(0,\gamma;\alpha,H,Re). \tag{3.17}$$

Once γ has been evaluated from (3.17) for any α, H and Re, the exact solution is given by (3.16).

3.1.3 Darcy-Brinkman-Forchheimer model

We also consider a steady state, pressure driven and fully developed unidirectional flow through a horizontal channel that is filled with porous media. This problem is well presented in [11, 59, 60]. The impermeable lower and upper walls of the channel are located at $y = -h$ and $y = h$ respectively. The flow is unidirectional in the $x - axis$ direction and hence the velocity of the fluid is of the form $v = (u(y), 0, 0)$. To model this phenomena we use the Darcy-Brinkman-Forchheimer momentum equations [11, 59, 60], given by

$$\frac{\mathrm{d}u^*}{\mathrm{d}y^{*^2}} = \frac{G}{-\mu_{eff}} + \frac{u^*}{MK} + \frac{\rho C_f}{\mu\sqrt{K}}u^{*^2}. \tag{3.18}$$

where C_f is the drag coefficient, G is the pressure gradient, K is the permeability, ρ is the fluid density, μ is the fluid viscosity, μ_{eff} is the viscosity of the fluid inside the the porous medium and $M = \frac{\mu}{\mu_{eff}}$ is the viscosity ratio. We then define dimensionless variables

$$y^* = yh, \quad u^* = \frac{Gh^2u}{\mu}. \tag{3.19}$$

Substituting (3.19) into (3.18), we get a dimensionless second order nonlinear governing Darcy-Brinkman-Forcheimer momentum equation

$$\frac{\mathrm{d}^2u}{\mathrm{d}y^2} - s^2u - Fsu^2 + \frac{1}{M} = 0, \tag{3.20}$$

subject to the symmetry boundary conditions

$$u(-1) = 0 \quad u(1) = 0. \tag{3.21}$$

where the porous medium shape parameter s, the Forchheimer number F and Darcy number are defined by

$$s = \frac{1}{\sqrt{MDa}}, \quad F = \frac{C_f\rho Gh}{\mu_{eff}\mu}, \quad Da = \frac{K}{h^2}. \tag{3.22}$$

3.2 Methods of solution

In this section we present a brief outline of the implementation of the ADM and SADM. We further reveal the modification of the SADM, the MSADM. Lastly, we shall reveal the the procedure to test convergence and rate of convergence of the presented methods of solution. Let us consider the most general non linear ordinary differential equation of the form:

$$Hy(x) + Fy(x) = g(x). \tag{3.23}$$

Here H is the linear ordinary differential operator consisting all the linear terms. On another note, F is a non linear ordinary differential operator combining all the non linear terms and g is a known function of x.

3.2.1 Adomian Decomposition method

Here we illustrate the implementation of the ADM on the general equation (3.23) in accordance to Adomian [79]. The linear ordinary differential term Hy, is decomposed into $Ly + Ry$ such that equation (3.23) becomes

$$Ly + Ry + Fy = g(x). \tag{3.24}$$

In principle, L denotes the highest order derivative amongst the linear terms. However, for singular problems L combines both the highest order derivative and the singularity terms. This definition of L makes it easier to find the inverse integral operator L^{-1}. R is the rest of the linear operator of order less than L. Since the inverse of L exists, then solving for y in (3.24) we come up with the following equation

$$L^{-1}Ly = L^{-1}g(x) - L^{-1}Ry - L^{-1}Fy. \tag{3.25}$$

The definition of L^{-1} depends on the type of the differential equation. If we have an initial value problem then the integral operator L^{-1} is given by a

sequence of definite integrals from x_0 to x. If L is an n^{th} order operator then L^{-1} will be an $n-$fold integration operator. Hence

$$L^{-1}Ly = y - \sum_{m=0}^{n-1} \frac{y^{(m)}(x_0)}{m!}(x - x_0)^m. \tag{3.26}$$

However, for boundary value problems indefinite integrals are used. Such that,

$$L^{-1}Ly = y - \sum_{m=0}^{n-1} \frac{\alpha_m}{m!}x^m. \tag{3.27}$$

To solve for the integration constants α_m we use the given boundary conditions. This approach may also be used in the case of initial value problems. Substituting (3.27) into (3.25) we get

$$y = \sum_{m=0}^{n-1} \frac{\alpha_m}{m!}x^m + L^{-1}g(x) - L^{-1}Ry - L^{-1}Fy. \tag{3.28}$$

With the Adomian decomposition method, the unknown function $y(x)$ is defined using an infinite series

$$y(x) = \sum_{n=0}^{\infty} y_n(x). \tag{3.29}$$

Also, the non linear function $F(y)$ is approximated using an infinite series of special polynomials

$$F(y) = \sum_{n=0}^{\infty} A_n. \tag{3.30}$$

A_n are the Adomian decomposition polynomials of $y_0, y_1, y_2, ..., y_n$ given by

$$A_n = \frac{1}{n!}\frac{d^n}{d\lambda^n}\left[F\left(\sum_{i=0}^{n}\lambda^i y_i\right)\right]_{\lambda=0}. \tag{3.31}$$

Substituting (3.29) and (3.30) into equation (3.28) we come out with the following iterative scheme

$$y_0(x) = \sum_{m=0}^{n-1} \frac{\alpha_m}{m!}x^m + L^{-1}g(x),$$
$$y_{n+1}(x) = -L^{-1}Ry_n - L^{-1}A_n,\ n = 0, 1, 2, ...$$

Solving the above scheme we may recursively compute the components $y_0, y_1, y_2, ..., y_n$ of $y(x)$.

3.2.2 Spectral Adomian Decomposition method

For the Spectral Adomian decomposition method, we define L in such a way that it is equivalent to H. In light of the latter, rearranging equation (3.23) we get

$$Ly(x) = g(x) - Fy(x). \tag{3.32}$$

Substituting (3.29) and (3.30) into (3.32) gives

$$L\sum_{n=0}^{\infty} y_n(x) = g(x) - \sum_{n=0}^{\infty} A_n. \tag{3.33}$$

Assuming that $Ly_0(x) = g(x)$, we come out with the recurrence relation

$$Ly_0(x) = g(x), \tag{3.34}$$

$$Ly_{n+1}(x) = -A_n,\ n = 0, 1, 2, ... \tag{3.35}$$

which we may solve to get the components $y_0, y_1, y_2, ..., y_n$ of $y(x)$.

However, from the definition of L, it is clear that sometimes L may be too difficult if not impossible to calculate analytically for some differential equations. Such differential equations are those that have more than one linear terms with the exception of singular ones. Our test samples are not an exception. As a result L^{-1} may not exist. For that matter, we employ a numerical procedure called the Chebyshev spectral collocation method to approximate L. This makes it easier to calculate L^{-1} and further solve for each y_n in (3.35). A brief outline of the pseudo spectral collocation method has been given in Chapter 2. More details of the spectral method are given in [77, 78].

3.2.3 Modified SADM

We illustrate a simple alteration of the SADM that remarkably improves the speed of convergence of the SADM for solving (3.32). This altered iterative scheme will be referred hereafter as the modified SADM abbreviated MSADM. Using the same initial guess ($y_0(x)$) obtained by solving (3.34), we define the following transformation

$$y(x) = y_0(x) + u(x). \tag{3.36}$$

Before we solve the governing equation (3.32), we first transform it and its boundary conditions using (3.36). The new equation becomes

$$L_1(u(x)) - F_1(u(x)) = f(x). \tag{3.37}$$

where L_1 and F_1 are linear and non linear operators respectively. The corresponding transformed boundary conditions will be always homogeneous. We then solve the above equation (3.37) using the standard SADM as discussed in previous sections. We will end up with the following iterative scheme

$$L_1(u_0(x)) = f(x), \tag{3.38}$$

$$L_1(u_{r+1}(x)) = A_r, \quad r = 0, 1, 2, 3, ... \tag{3.39}$$

which we solve using the pseudo spectral collocation method to get the components $u_0, u_1, u_2, ...$ of $u(x)$.

3.3 Test for convergence and numerical approximation of convergence rates and degree of accuracy

In this work, we are interested in giving an account about the performance of each iterative scheme based on convergence, rate of convergence and level accuracy of the numerical approximation. In this section we present the procedure used to compute the latter 3 variables. To test if the method converges we consider the infinite norm(e_i) at each i^{th} iteration. Each scheme converges if

$$e_i = \|y_* - y_i\|_\infty,$$

where y_* is the exact solution and y_i is the approximate solution of $y*$ at the i^{th} iteration. In short, the scheme converges if the infinity norms between successive iterations decreases with increase in the number of iterations i(i.e. $e_1 < e_2 < e_3 < ...$).

A method is said to converge with the rate p if

$$\lim_{i\to\infty} \frac{\|y_{i+1} - y_*\|_\infty}{\|y_i - y_*\|_\infty^p} = K, \tag{3.40}$$

where K is a positive finite constant. Equation (4.29) can be reduced to

$$\frac{e_{i+2}}{e_{i+1}} = \left(\frac{e_{i+1}}{e_i}\right)^p. \tag{3.41}$$

Taking natural logarithms on both sides of (4.30) we get the convergence rate p in explicit form:

$$p = \frac{\ln(e_{i+2}/e_{i+1})}{\ln(e_{i+1}/e_i)}. \tag{3.42}$$

where $e_{i+2},\ e_{i+1},\ e_i$ are infinite norms computed for three consecutive iterations.

It is worth mentioning at this stage that we will test the level of accuracy of the method by considering a simple absolute error between the approximate and exact solutions.

3.4 Numerical experiments

In this section we illustrate the application of each of the three methods of solution presented earlier on our sample problems.

3.4.1 Solution to Jeffery-Hamel problem by ADM

The MHD Jeffery-Hamel problem was solved in [32, 33, 34, 35] using the ADM as follows. In operator form the governing equation (3.6) becomes

$$Ly = (H-4)\alpha^2 y' - 2\alpha Reyy', \tag{3.43}$$

where

$$L(.) = \frac{\mathrm{d}^3(.)}{\mathrm{d}x^3}, \quad L^{-1}(.) = \int_0^x \int_0^x \int_0^x (.)\mathrm{d}x\mathrm{d}x\mathrm{d}x. \tag{3.44}$$

Applying the inverse operator on both sides of equation 3.43 and using the initial conditions $y(0) = 1$ and $y'(0) = 0$ we get

$$y = 1 + \frac{ax^2}{2} + L^{-1}(H-4)\alpha^2 y - L^{-1}2\alpha Reyy', \tag{3.45}$$

where $a = y''(0) \neq 0$ is not given but will be obtained by using the other boundary condition $y(1) = 0$. Substituting equations (3.29) and (3.30) into (3.45) we get

$$\sum_{n=0}^{\infty} y_n(x) = 1 + \frac{ax^2}{2} + L^{-1}\left((H-4)\alpha^2 \sum_{n=0}^{\infty} y_n\right) - L^{-1}\left(2\alpha Re \sum_{n=0}^{\infty} A_n\right), \tag{3.46}$$

where A_n are the Adomian decomposition polynomials that approximate the nonlinear term yy'. From equation (3.46), we set $y_0 = 1 + \frac{ax^2}{2}$ to obtain the following recurrence relation

$$y_{n+1} = L^{-1}\left((H-4)\alpha^2 y_n\right) - L^{-1}\left(2\alpha Re A_n\right), n = 0, 1, 2, 3, ... \tag{3.47}$$

We use this iterative scheme to solve for the remaining components of $y(x)$.

3.4.2 Solution to Jeffery-Hamel problem by SADM

In operator form the governing equation (3.6) becomes

$$Ly = -2\alpha Reyy', \tag{3.48}$$

where $L(.) = (\mathbf{D}^3 + (4-H)\alpha^2\mathbf{D})(.)$. Substituting equations (3.29) and (3.30) into (3.48) we get

$$L\sum_{n=0}^{\infty} y_n = -\sum_{n=0}^{\infty} 2\alpha Re A_n, \tag{3.49}$$

where A_n are the so called Adomian decomposition polynomials used to approximate the nonlinear term yy'. To identify the zeroth component y_0, from (3.49), we set

$$Ly_0 = \mathbf{P}, \tag{3.50}$$

where $\mathbf{P}$ is a zero column vector of size $N+1$. Consequently, from equation (3.49) we come up with the following iterative scheme

$$Ly_{n+1} = \mathbf{Q}_n, \quad n = 0, 1, 2, 3, ... \tag{3.51}$$

subject to

$$y_{n+1}(0) = 1, \quad y'_{n+1}(0) = 0, \quad y_{n+1}(1) = 0. \tag{3.52}$$

Here, $\mathbf{Q}_n,\ n = 0, 1, 2, 3, ...$ is a column vector of the values of $2\alpha Re A_n$ at the collocation points. We use this recurrence relation to determine the other

components $y_n,\ n = 1, 2, 3, ...$ of $y(x)$.

We remark that matrix L is of size $(N+1)\times(N+1)$ where $N+1$ is the number of collocation points. Under the Chebyshev spectral method , the Dirichlet boundary conditions are imposed on the first and last rows of L as follows. We substitute every element in these rows with zeros. The first zero on the first row together with the last zero on the last row are replaced by 1. The first and last elements of vector $\mathbf{P}$ are replaced by 0 and 1 respectively. The same is done on the first and last elements of $\mathbf{Q}$. To impose the boundary condition, $y'_{n+1}(0) = 0$ we replace the last but one row (N^{th} row) of L with the last row of $\mathbf{D}$. The N^{th} element of $\mathbf{P}$ and $\mathbf{Q}$ are replaced with zero.

3.4.3 Solution to Jeffery-Hamel problem by MSADM

Applying the transformation (3.36) into the system (3.6)-(3.7) we get

$$u''' + (2\alpha Rey_0 + (4 - H)\alpha^2)u' + 2\alpha Rey'_0 u + 2\alpha Reuu' = f(x) \tag{3.53}$$

subject to the boundary conditions

$$u(0) = 0, \quad u'(0) = 0 \quad u(1) = 0. \tag{3.54}$$

where$f(x) = -(y'''_0 + 2\alpha Rey_0 y'_0 + (4 - H)\alpha^2 y'_0)$ and y_0 is the solution to equation (3.50).

In operator form the governing equation 3.53 becomes

$$L_1 u(x) = -2\alpha Reuu' + f(x), \tag{3.55}$$

where $L_1(.) = \left[\mathbf{D}^3 + [2\alpha Rey_0 + (4 - H)\alpha^2]\,\mathbf{D} + diag(2\alpha Rey'_0)\right](.)$.

Substituting equations (3.29) and (3.30) into (3.65) we get

$$L_1 \sum_{n=0}^{\infty} u_n = -\sum_{n=0}^{\infty} 2\alpha ReA_n + f(x), \tag{3.56}$$

where A_n are the so called Adomian decomposition polynomials used to approximate the nonlinear term uu'. From (3.56), we set

$$L_1 u_0(x) = f(x), \tag{3.57}$$

to identify the zeroth component u_0. Consequently, from equation (3.56) we come up with the following iterative scheme

$$L_1 u_{n+1}(x) = -2\alpha Re A_n, \quad n = 0, 1, 2, 3, ... \tag{3.58}$$

subject to the following boundary conditions

$$y_{r+1}(0) = 0, \quad y'_{r+1}(0) = 0, \quad y_{r+1}(1) = 0. \tag{3.59}$$

We use this recurrence relation to determine the other components $u_n(x),\ n = 1, 2, 3, ...$ of $u(x)$.

We remark that the resultant boundary conditions in (3.59) are homogeneous. These boundary conditions are implemented exactly the same way as we imposed those in (3.52) on the SADM iterative scheme under Section 3.4.2.

3.4.4 Solution to Darcy-Brinkman-Forhheimer model by ADM

A demonstration on how the ADM is used to solve the Darcy-Brinkman-Forchheimer model is shown in this section. In operator form the governing equation (3.20) becomes

$$Lu(y) = -\frac{1}{M} + s^2 u(y) + Fsu^2(y), \tag{3.60}$$

where

$$L(.) = \frac{\mathrm{d}^2(.)}{\mathrm{d}y^2}, \quad L^{-1}(.) = \int_{-1}^{y}\int_{-1}^{y}(.)\,\mathrm{d}y\,\mathrm{d}y. \tag{3.61}$$

Applying the inverse operator on both sides of equation (3.60) and using the initial condition $u(-1) = 0$ we get

$$u = a(u+1) - L^{-1}\left(\frac{1}{M}\right) + L^{-1}(s^2 u) + L^{-1}(Fsu^2), \tag{3.62}$$

where $a = y'(-1) \neq 0$ is not given but will be obtained by using the other boundary condition. Substituting equations (3.29) and (3.30) into (3.62) we get

$$\sum_{n=0}^{\infty} u_n(y) = a(y+1) - L^{-1}\left(\frac{1}{M}\right) + L^{-1}\left(s^2 \sum_{n=0}^{\infty} u_n\right) + L^{-1}\left(Fs \sum_{n=0}^{\infty} A_n\right), \tag{3.63}$$

where A_n are the Adomian decomposition polynomials that approximate the nonlinear term u^2. From equation (3.63), we set $u_0 = a(y+1) - L^{-1}\left(\frac{1}{M}\right)$ to obtain the following recurrence relation

$$u_{n+1} = L^{-1}\left(s^2 u_n\right) + L^{-1}\left(FsA_n\right), n = 0, 1, 2, 3, ... \tag{3.64}$$

We use this iterative scheme to solve for the remaining components of $u(x)$.

3.4.5 Solution to Darcy-Brinkman-Forhheimer model by SADM

In operator form the governing equation (3.20) becomes

$$Lu(y) = -\frac{1}{M} + Fsu^2(y), \tag{3.65}$$

where $L = \mathbf{D}^2 - diag(s^2)$. Substituting equations (3.29) and (3.30) into (3.65) we get

$$L\sum_{n=0}^{\infty} u_n(y) = -\frac{1}{M} + \sum_{n=0}^{\infty} FsA_n, \tag{3.66}$$

where A_n are the so called Adomian decomposition polynomials used to approximate the nonlinear term $u^2(y)$. From (3.66), we set

$$Lu_0(y) = -\frac{1}{M} \tag{3.67}$$

to identify the zeroth component $u_0(y)$. Consequently, from equation (3.66) we come up with the following iterative scheme

$$Lu_{n+1}(y) = FsA_n, \quad n = 0, 1, 2, 3, ... \tag{3.68}$$

subject to

$$u_{n+1}(-1) = 0, \quad u_{n+1}(1) = 0. \tag{3.69}$$

We use this recurrence relation to determine the other components $u_n(y),\ n = 1, 2, 3, ...$ of $u(y)$.

3.4.6 Solution to Darcy-Brinkman-Forhheimer model by MSADM

Applying the transformation (3.36) into the system (3.20)-(3.21) we get

$$U'' - \left(s^2 + 2Fsu_0\right) U - FsU^2 = f(y) \tag{3.70}$$

subject to the boundary conditions

$$U(-1) = 0, \quad U(1) = 0. \tag{3.71}$$

where $f(y) = -u_0'' + 2s^2u_0 + Fsu_0^2 - \frac{1}{M}$ and u_0 is obtained as a solution to equation (3.67).

In operator form the governing equation (3.70) becomes

$$L_1U = FsU^2 + f(y), \tag{3.72}$$

where $L_1(.) = \left[\mathbf{D}^2 - (s^2 + 2Fsdiag(u_0))\right](.)$.

Substituting equations (3.29) and (3.30) into (3.72) we get

$$L_1 \sum_{n=0}^{\infty} U_n = -\sum_{n=0}^{\infty} FsA_n + f(y), \tag{3.73}$$

where A_n are the so called Adomian decomposition polynomials used to approximate the nonlinear term U^2. From (3.73), we set

$$L_1 U_0 = f(y), \tag{3.74}$$

to identify the zeroth component U_0. Consequently, from equation (3.73) we come up with the following iterative scheme

$$L_1 U_{n+1}(x) = FsA_n, \quad n = 0, 1, 2, 3, ... \tag{3.75}$$

subject to

$$U_{n+1}(-1) = 0, \quad U_{n+1}(1) = 0. \tag{3.76}$$

3.5 Presentation and discussion of results

Here, we discuss the results obtained when applying the ADM, SADM and MSADM concurrently, for solving the MHD Jeffery-Hamel flow model and the Darcy-Brinkman-Forchheimer momentum equations. Table 3.1 shows the number of iterations taken by the MSADM, ADM and SADM to match the exact solution of $y''(0)$ by up to 35 decimals. The governing parameters H, Re and α of the MHD Jeffery-Hamel problem were set to be $0, 10, -30^0$ respectively. The absolute error at each iteration is captured for all the iterative schemes.

Table 3.1: Comparison of the minimum number of iterations required by each method to match the exact solution of $y''(0)$ by up to 35 decimals

.

$H = 0, Re = 10, \alpha = -5^o$ exact $-1.78454677114046075818783060639084633 3$		
Order	$y''(0)$	Absolute Errors
	MSADM	
3	-1.78454677114125587131494715899161980 2	7.951×10^{-13}
6	-1.78454677114046075817923173835589072 8	8.599×10^{-21}
9	-1.78454677114046075818783060650815837 3	1.173×10^{-28}
12	-1.78454677114046075818783060639084633 1	1.800×10^{-36}
	ADM	
3	-1.78454657693497997987438666835276073 6	1.942×10^{-7}
6	-1.78454677114312885030709139371472409 5	2.668×10^{-12}
9	-1.78454677114046078664070043685944644 9	2.845×10^{-17}
12	-1.78454677114046075818452965845399470 7	3.301×10^{-21}
15	-1.78454677114046075818783074354845359 3	1.372×10^{-25}
18	-1.78454677114046075818783060638653720 8	4.309×10^{-30}
22	-1.78454677114046075818783060639084633 5	2.113×10^{-36}
	SADM	
3	-1.78455110195546399630814196512632989 1	4.331×10^{-6}
6	-1.78454677218568490254025876702164321 1	1.045×10^{-9}
9	-1.78454677114069377664679175704516714 7	2.330×10^{-13}
12	-1.78454677114046080908441830460303615 5	5.090×10^{-17}
15	-1.78454677114046075819876347880128324 6	1.093×10^{-20}
18	-1.78454677114046075818783290570383678 7	2.299×10^{-24}
22	-1.78454677114046075818783060638398884 9	6.857×10^{-30}
25	-1.78454677114046075818783060639084633 9	5.939×10^{-35}

From Table 3.1, the 12^{th} order MSADM is required to give an approximate solution of $y''(0)$ that matches the exact solution by up to 36 decimals. In this discussion, the number of iterations and order of the iterative schemes are used interchangeably since they both indicate the number of the components $y_0(x), y_1(x), y_2(x), \ldots, y_M(x)$ used in the series solution of $y(x)$. Under the same conditions, the ADM took 22 iterations followed by the SADM with 25 iterations to generate an approximate solution of the required level of accuracy. Its worth observing that as we increase the order for each method the level of accuracy also increases. The MSADM is more efficient than the ADM and SADM since it took lesser number of iterations to converge to within 35 digits accuracy.

The absolute errors for corresponding different number of collocation points (N) used and various order (M) of the MSADM is shown in Table 3.2. The indicated absolute errors are with respect to the exact solution of $y''(0)$ of the MHD Jeffery-Hamel flow problem when $H = 0$, $Re = 100$ and $\alpha = -5^o$.

Table 3.2: The absolute errors for the solution of $y''(0)$ corresponding to different number of collocation points (N) and varying order (M) of the MSADM.

$H = 0, Re = 100, \alpha = -5^o$, exact $= -0.640178117359539137672473914980$.				
N	M			
	10^{th}	20^{th}	30^{th}	35^{th}
20	8.721×10^{-8}	8.719×10^{-8}	8.719×10^{-8}	8.719×10^{-8}
30	1.680×10^{-11}	6.723×10^{-14}	6.723×10^{-14}	6.723×10^{-14}
40	1.674×10^{-11}	2.998×10^{-19}	2.671×10^{-20}	2.671×10^{-20}
50	1.674×10^{-11}	2.730×10^{-19}	1.329×10^{-26}	7.140×10^{-27}
60	1.674×10^{-11}	2.730×10^{-19}	6.152×10^{-27}	9.794×10^{-31}
70	1.674×10^{-11}	2.730×10^{-19}	6.152×10^{-27}	9.808×10^{-31}
80	1.674×10^{-11}	2.730×10^{-19}	6.152×10^{-27}	9.808×10^{-31}
90	1.674×10^{-11}	2.730×10^{-19}	6.152×10^{-27}	9.808×10^{-31}
100	1.674×10^{-11}	2.730×10^{-19}	6.152×10^{-27}	9.808×10^{-31}
150	1.674×10^{-11}	2.730×10^{-19}	6.152×10^{-27}	9.808×10^{-31}
200	1.674×10^{-11}	2.730×10^{-19}	6.152×10^{-27}	9.808×10^{-31}

Clearly, for each number of grid points (N) used, the level of accuracy of the series solution increases with increase in the order (M) of the MSADM. However the latter relation is false for each order. As we increase the number of grid points for a particular order, there exists an optimal value of (N) such that further increase of the number of collocation points does not improve the level of accuracy of the solution. For example, for the 30^{th} order MSADM, further increase of N beyond 60 does improve the accuracy of the solution.

Table 3.3 shows the comparison of the MSADM and SADM approximate solutions against the exact solutions of $y''(0)$ for different values of Re. The values of H and α are fixed. The tolerance level used by the MSADM and SADM is around 10^{-21} and 10^{-13} respectively. The table also demonstrates the effect of varying the Reynolds number on the convergence speed for both methods. The results are also validated against literature results and `bvp4c`.

Table 3.3: Comparison between the MSADM and SADM results against the exact values of $y''(0)$ for different values of Reynolds numbers when $H = 0$, $\alpha = -5^o$

Re	Iter.	$y''(0)$	Abs. error	Time(s)
		MSADM		
10	6	-1.78454677114046075819	8.599×10^{-21}	2.636
20	9	-1.58815348501763196214	1.342×10^{-22}	7.083
30	10	-1.41369208398850773163	7.335×10^{-21}	9.641
40	12	-1.25899391695680932384	3.383×10^{-21}	18.704
50	14	-1.12198914667456548041	1.800×10^{-21}	32.838
60	16	-1.00074264847743489433	1.167×10^{-21}	55.615
		SADM		
10	9	-1.7845467711407	2.330×10^{-13}	5.414
20	11	-1.588153485018	7.197×10^{-13}	8.72
30	14	-1.413692083988	9.843×10^{-14}	21.918
40	17	-1.258993916956	5.977×10^{-13}	44.804
50	22	-1.121989146674	1.244×10^{-13}	118.904
60	25	-1.000742648477	1.904×10^{-13}	257.184

Re	Exact: $y''(0)$	Error in [84]	`bvp4c`
10	-1.78454677114046075818	6.944×10^{-8}	-1.784546771140456
20	-1.58815348501763196214	5.198×10^{-8}	-1.588153485017627
30	-1.41369208398850773163	6.055×10^{-8}	-1.413692083988505
40	-1.25899391695680932384	1.813×10^{-8}	-1.258993916956809
50	-1.12198914667456548041	1.031×10^{-7}	-1.121989146674567
60	-1.00074264847743489433	2.791×10^{-7}	-1.000742648477438

From Table 3.3, the MSADM took 6 iterations to converge to within 21 digits accuracy when $Re = 10$. We note that as we increase the value of Re, the number of iterations also increases to get results of the same degree of accuracy. This relationship between Re and the number of iterations also holds for the SADM. The MSADM took 16 iterations to generate an approximate solution that matches the exact solution by 21 decimals for $Re = 60$. For the same value of Re it required the SADM of order 25 to give a solution that is in agreement with the exact solution by only 13 decimal values. Consequently, we may say that the MSADM is more computationally efficient than the SADM. This is true for all Re. It is worth mentioning that the lesser the number of iterations is used by each method the lesser the amount of run time is required. Based on the latter, the MSADM is more efficient than the SADM since it reaches higher level of accuracy than SADM using only a few iterations. However, both methods seem to have produced more accurate results for each respective Re when compared against literature results by Abbasbandy and Shivanian [84].

Table 3.4 shows the effect of increasing the Hartmann number(H) on the speed of convergence for the SADM and MSADM. We considered a divergent channel for a fixed value of $Re = 10$. Both SADM and MSADM results are validated against Numerical results by `bvp4c` in this case.

Table 3.4: Comparison between the SADM and ASADM results against numerical values of $y''(0)$ for different values of H when $Re = 10,\ \alpha = 5^o$.

H	Order	$y''(0)$	Abs. Error
		SADM	
200	9	-1.9846061833010	8.837×10^{-14}
600	9	-1.5546060373980	3.819×10^{-14}
1000	9	-1.2304372999737	4.174×10^{-14}
2000	8	-0.7125849888716	9.603×10^{-14}
3000	8	-0.4316079639073	1.08×10^{-13}
4000	7	-0.2709018858119	1.716×10^{-13}
5000	7	-0.1750443192237	7.622×10^{-14}
		MSADM	
200	4	-1.9846061833009	5.107×10^{-15}
600	4	-1.5546060373980	1.177×10^{-14}
1000	3	-1.2304372999737	7.394×10^{-14}
2000	3	-0.7125849888716	8.837×10^{-14}
3000	2	-0.4316079639081	6.558×10^{-13}
4000	2	-0.2709018858117	4.258×10^{-14}
5000	2	-0.1750443192236	1.152×10^{-13}
H	`bvp4c`	[**85**]	[**84**]
200	-1.98460618330090	-1.9846062	-1.984606164603458
600	-1.55460603739805	-1.5546060	-1.554605992057426
1000	-1.23043729997374	-1.2304373	-1.230437181792459
2000	-0.71258498887168	-0.7125850	-0.712584949074417
3000	-0.43160796390742	-0.4316080	-0.431607723269544
4000	-0.27090188581172	-0.2709019	-0.270901503198049
5000	-0.17504431922376	-0.1750443	-0.175043638247544

We notice that as we increase H the speed of convergence by each method accelerates. When $H = 200$ we used the SADM of order 9 to match the numerical results by 14 decimals. However when $H = 5000$ only 7 iterations were required to achieve the same level of accuracy by the SADM. Still the MSADM proves to converge faster than the SADM since it takes a relatively less number of iterations to converge to the same level of accuracy as the SADM. Furthermore, the SADM and MSADM are more accurate than methods found in literature. The SHAM by Motsa et al. [85] and results by Abbasbandy and Shivanian [84] matched the numerical solution by only 8 decimals.

Table 3.5 shows the ADM solution for $u(0)$ of the Darcy-Brinkman-Forhheimer model for varying values of the governing physical constants. The solution of $u(0)$ by the $10^t h$ and 20^{th} order ADM is compared against the Numerical results generated by `bvp4c`.

Table 3.5: Comparison between ADM results for $u(0)$ with `bvp4c` for varying F, M, and s.

.

F	M	s	**ADM**		`bvp4c`
			$10^{th}Order$	$20^{th}Order$	
1	1	1	0.3238524531882	0.3238524135166	0.323852413516572
1.2	1	1	0.3191635104506	-	0.319163416932828
1.8	1	1	0.3064562749516	-	0.306455613892256
2	1	1	0.3026103113364	-	0.302609205103015
1	2	1	0.1684008983035	0.168400897388858	0.168400897388857
1	3	1	0.1138578100870	0.113857809969176	0.113857809969175
1	4	1	0.0860143805098	0.086014380480271	0.086014380480270
1	1	2	0.1745385431549	0.1744325862905	0.174432545071645
1	1	3	-5.0270028440209	-5.0049549340474	0.097565017666643
1	1	4	-5.1396479412378	-4.8776924415183	0.059421335718288
Run time(s):			**2864.83**	**44806.1**	

From Table 3.5, we observe that when $s >> 2$, the 10^{th} order ADM does not converge to the correct solution. An attempt to improve the results by employing the ADM of order 20 was futile. As a result, the ADM lacks robustness and reliability since it is selective on the values of some governing physical constants. The dashes (-) under the ADM of order 20 indicates that, for those combinations of F, M and s, the solutions by the ADM could not be captured. The ADM iterative scheme was terminated after running for days without giving the solutions. From the table, this may be as result of increasing F beyond 1. The slow convergence speed of the ADM can also

be attributed to its semi analytical nature. The 44 806.1 seconds recorded under the 20^{th} order ADM is the time it took to compute the captured results. The ADM seems to be not sensitive on the values of M only. Apart from the cases where $s > 2$ and when $F > 1$, the solution by the 20^{th} order ADM matched `bvp4c` by 14 decimal digits. This is a very excellent level of accuracy. However, the lack of consistency in all the different values of the governing parameters makes the ADM an incompetent method.

Table 3.6 shows the initial solutions for the Darcy-Brinkman-Forchheimer momentum equation, corresponding to varying governing parameters. The $u(0)$ solutions were obtained using the MSADM and the SADM. The different values of the governing constants $(F\ , M\ , s)$ are exactly the same as those used by the ADM in Table 3.5 for the same solution. The number of iterations taken by the MSADM and SADM to converge to the solution is shown.

Table 3.6: The solutions by SADM and MSADM for $u(0)$ for varying F, M, and s.

.

F	M	s	Order	$u(0)$	Abs. Err.
				MSADM	
1	1	1	6	0.323852413516575	2.665×10^{-15}
1.2	1	1	7	0.319163416932829	1.221×10^{-15}
1.8	1	1	8	0.306455613892265	8.937×10^{-15}
2	1	1	9	0.302609205103018	3.164×10^{-15}
1	2	1	4	0.168400897388863	5.551×10^{-15}
1	3	1	4	0.113857809969176	1.374×10^{-15}
1	4	1	3	0.086014380480272	1.846×10^{-15}
1	1	2	5	0.174432545071648	3.22×10^{-15}
1	1	3	3	0.097565017666649	5.773×10^{-15}
1	1	4	3	0.059421335718291	2.928×10^{-15}
Run time(s):				**8.563**	
				SADM	
1	1	1	24	0.323852413516580	8.382×10^{-15}
1.2	1	1	29	0.319163416932820	7.938×10^{-15}
1.8	1	1	55	0.306455613892251	5.44×10^{-15}
2	1	1	71	0.302609205103009	5.995×10^{-15}
1	2	1	15	0.168400897388857	3.331×10^{-16}
1	3	1	12	0.113857809969178	2.554×10^{-15}
1	4	1	10	0.086014380480274	4.149×10^{-15}
1	1	2	16	0.174432545071651	5.634×10^{-15}
1	1	3	11	0.097565017666645	1.568×10^{-15}
1	1	4	8	0.059421335718293	5.246×10^{-15}
Run time(s):				**29.017**	

From Table 3.6, both the SADM and MSADM were able to converge to the solutions of $u(0)$ for each of the various governing physical parameters. An excellent and acceptable level of accuracy was demonstrated by the SADM and MSADM by matching the numerical solution by 15 decimal digits. The latter is justified by the absolute errors shown in the table. Furthermore the MSADM is indeed an improvement of the SADM since it used lesser number of iterations to converge to the same level of accuracy as the SADM for each various constants. It takes the SADM of order 11 and 8 to converge to the numerical solution by up to 15 decimals for s equals to 3 and 4, respectively. The MSADM took 3, 3 and 2 iterations to converge to the same level of accuracy when s is equals to 3, 4 and 5 respectively. Quite remarkably, an increase in s corresponds to a decrease in the order of the SADM and MSADM required to attain a certain level of accuracy. However, for the same values of s, the ADM of order 20 could not converge even by a single decimal to the numerical solution of $u(0)$. It took the MSADM almost 9 seconds to compute the solution of the Darcy-Brinkman-Forchheimer problem for all the varying values of $F,\ M,\ s$ whilst the SADM took around 30 seconds. According to Table 3.5, the ADM of order 10 took around 2900 seconds to solve the problem for all the varied physical parameters. Not only did the ADM take long, it also produced poorer solutions than the SADM and MSADM, in terms of accuracy.

Table 3.7 and 3.8, shows the comparison of the performance amongst the ADM, SADM and MSADM in finding the solution to the Darcy-Brinkman-Forchheimer problem. The tables show the values of $u'(1)$ for each unique set of varied governing parameters. The time taken by the ADM, SADM and MSADM during their computations is also shown. Table 3.7 shows the solution of $u'(1)$ by the ADM of order 10 and 20. The solution by each of the

three methods is compared against `bvp4c` results that are given in Table 3.7. Similarly, Table 3.8 shows the solutions of $u'(1)$ generated by the MSADM and SADM. In this table, the absolute error to each solution is shown.

Table 3.7: Comparison between ADM results for $u'(1)$ with `bvp4c` for varying F, M, and s.

.

F	M	s	**ADM**		`bvp4c`
			$10^{th}Order$	$20^{th}Order$	
1	1	1	0.7212354973126	0.7212354658900	0.721235465889991
1.2	1	1	0.7144594552926	-	0.714459382175989
1.8	1	1	0.6960315562197	-	0.696031058075487
2	1	1	0.6904344356150	-	0.690433611674491
1	2	1	0.3699435954331	0.3699435946833	0.369943594683339
1	3	1	0.2489128381568	0.2489128380591	0.248912838059091
1	4	1	0.1875752289483	0.1875752289237	0.187575228923653
1	1	2	0.4691832004788	0.4691286749495	0.469128653738031
1	1	3	-4.6582674518929	-5.0179976531010	0.328027760431911
1	1	4	-6.3730387384123	-6.8579531834296	0.248573640072203
Run time(s):			**2864.83**	**44806.1**	

Table 3.8: The SADM and MSADM results for $u'(1)$ corresponding to varying F, M, and s.

.

F	M	s	Order	$u(0)$	Abs. Err.
				MSADM	
1	1	1	6	0.721235465890000	8.882×10^{-15}
1.2	1	1	7	0.714459382175999	9.992×10^{-15}
1.8	1	1	10	0.696031058075491	3.664×10^{-15}
2	1	1	9	0.690433611674499	7.772×10^{-15}
1	2	1	5	0.369943594683346	7.272×10^{-15}
1	3	1	4	0.248912838059095	3.691×10^{-15}
1	4	1	3	0.187575228923657	4.191×10^{-15}
1	1	2	5	0.469128653738034	2.942×10^{-15}
1	1	3	3	0.328027760431915	3.83×10^{-15}
1	1	4	3	0.248573640072204	7.216×10^{-16}
Run time(s):				**8.563**	
				SADM	
1	1	1	25	0.721235465889993	1.554×10^{-15}
1.2	1	1	29	0.714459382175992	2.887×10^{-15}
1.8	1	1	53	0.696031058075484	3.442×10^{-15}
2	1	1	71	0.690433611674486	4.663×10^{-15}
1	2	1	15	0.369943594683344	5.218×10^{-15}
1	3	1	12	0.248912838059096	5.301×10^{-15}
1	4	1	10	0.187575228923660	7.355×10^{-15}
1	1	2	16	0.469128653738037	5.884×10^{-15}
1	1	3	11	0.328027760431911	3.331×10^{-16}
1	1	4	8	0.248573640072206	2.859×10^{-15}
Run time(s):				**29.023**	

The comparison between the ADM, SADM and MSADM in Table 3.7 and Table 3.8 does not change from what we observed in Table 3.5 and Table 3.6 earlier on. In Table 3.7, the ADM could not converge for values of s greater than 2. With the other combinations of the governing physical parameters, the ADM of order 10 still converges by only 6 decimal digits accuracy in 2864.83 seconds. This level of accuracy is very poor when compared with the 15 digits accuracy achieved using the MSADM and SADM in Table 3.8. The attempt to improve the 6 decimals digits accuracy by increasing the number of iterations to 20 was in vain for $s > 2$ and $F > 1$. From Table 3.8, the SADM and MSADM managed to compute the solution of $u'(0)$ for all the different combinations of the values of the governing physical parameters.

Chapter 4

The RQLM and its SADM-based higher order iterative schemes

In this chapter we present the construction of another new iterative method called the reduced quasilinearisation method (RQLM) and its SADM-based higher order iteration schemes for the numerical solution of a certain type of singular second order nonlinear two point boundary value problems (BVPs). The targeted class of nonlinear singular BVPs is of the form:

$$y''(x) + \frac{m}{x}y'(x) + f(y(x)) = 0, \quad x \in (0, 1] \tag{4.1}$$

subject to the boundary conditions

$$y'(0) = 0, \quad Ay(1) + By'(1) = C, \quad A > 0, B, C \geq 0. \tag{4.2}$$

Here, $f(y(x))$ is a nonlinear continuous function such that $\frac{\partial f}{\partial y}$ exists. Systems such as (4.1)-(4.2) have received much attention due to their vast applications in the study of tumor growth in physiology [61, 62]. Ford et al. [69]

proved the existence and uniqueness of the solution to this class of non linear singular BVPs. Many numerical treatments for this class of non linear singular BVPs have been presented in recent years. To mention a few, Motsa and Sibanda [70] employed the successive linearisation method to solve a class of singular nonlinear BVPs similar to equation (4.1). Their method proved to be more accurate than the literature results in [71, 72, 73, 74]. Çaglar et al. [71] used third-degree B-spline functions and the Levenberg-Marquardt optimisation method to approximate the solution to this class of BVPs. They tested their approach on a sample of three physical model problems: (i) thermal explosions, (ii) oxygen diffusion, and (iii) the non-linear heat conduction model of the human head. Their approach approximated the solutions very well. Abukhaled et al. [73] employed cubic B-splines to find approximate solutions of the singular two point boundary value problem (4.1)-(4.2). To remove the singularity at the origin, they used two approaches: L'Hospital's rule and an economised Chebyshev polynomial in the vicinity of the singular point. Their approach was more accurate when compared against the finite difference technique used by Pandey and Singh [72]. More studies around this class of non-linear singular ordinary differential equations arising in physiology have been conducted using the cubic B-spline collocation technique [75]. Rashidinia et al. [74] used a non-polynomial cubic spline method and tridiagonal solver to solve this class of non-linear singular ordinary differential equations after applying the quasilinearisation technique. Computational results showed that their approach is viable.

The applicability of the RQLM and its SADM-based higher order iterative schemes is tested on two physical problem models. These models are: (i) the thermal distribution in the human head, (ii) Oxygen diffusion in spherical cells. The method is also tested on a class of singular second order BVP with

an exact solution. The comparison between the QLM and RQLM SADM-based higher order schemes is made in terms of the accuracy and convergence rates of the approximate solutions. The validity of the obtained solutions is verified by the `bvp4c` results and the exact solution where applicable. Tables and graphs will be used to exhibit the comparisons.

4.1 Derivation of the iterative schemes

The QLM basically employs the Taylor series expansion of order 1 as a tool to linearize the nonlinear function $f(x, y)$ of the BVP. The resultant iterative scheme becomes linear. Evaluating all derivatives of the non linear function at initial approximation gives birth to the new generalised RQLM iterative scheme. The resultant linear iterative schemes will be solved using the pseudo spectral collocation method.

Following the approach by Motsa and Sibanda [88], we assume that $y_\alpha(x)$ is the exact solution of the governing equation (4.1) and that $y_\gamma(x)$ is an initial approximation that is sufficiently close to $y_\alpha(x)$. Upon linearising f using Taylor series expansion of up to first order about y_γ we obtain the following coupled system

$$y'' + \frac{m}{x}y' + f(y_\gamma) + (y - y_\gamma)\frac{\partial f}{\partial y}(y_\gamma) + g(y) = 0 \tag{4.3}$$

$$g(y) = f(y) - f(y_\gamma) - (y - y_\gamma)\frac{\partial f}{\partial y}(y_\gamma). \tag{4.4}$$

It is worth noting that adding equation (4.3) and (4.4) gives the governing equation (4.1). Re-arranging equation (4.3) we get

$$y'' + \frac{m}{x}y' + y\frac{\partial f}{\partial y}(y_\gamma) + g(y) = \Phi(y_\gamma), \tag{4.5}$$

where

$$\Phi(y_\gamma) = y_\gamma\frac{\partial f}{\partial y}(y_\gamma) - f(y_\gamma). \tag{4.6}$$

In operator form, equation (4.5) can be re-written as follows

$$\mathcal{L}y = \Phi(y_\gamma) + F(y) \tag{4.7}$$

where

$$\mathcal{L}y = y'' + \frac{m}{x}y' + y\frac{\partial f}{\partial y}(y_\gamma), \text{ and } F(y) = -g(y). \tag{4.8}$$

Here it is assumed that $F(y)$ is a nonlinear function and is decomposed using the Adomnian decomposition method (ADM) as

$$F(y) = \sum_{n=0}^{\infty} A_n, \tag{4.9}$$

where $A_n,\ n = 1, 2, 3, \ldots$ denote the Adomian functions that can be calculated for various classes of nonlinearity according to algorithms set out by Adomian [79, 80, 81] and Wazwaz [82, 83]. For a nonlinear function $F(y)$, the first few polynomials are given by

$$\begin{aligned} A_0 &= F(y_0), \\ A_1 &= y_1 F_y(y_0), \\ A_2 &= y_2 F_y(y_0) + \frac{y_1^2}{2!}F_{yy}(y_0), \\ A_3 &= y_3 F_y(y_0) + y_1 y_2 F_{yy}(y_0) + \frac{y_1^3}{3!}F_{yyy}(y_0). \end{aligned}$$

In the ADM, the solution $y(x)$ is also represented by an infinite series of the form

$$y(x) = \sum_{n=0}^{\infty} y_n(x). \tag{4.10}$$

Substituting equations (4.9) and (4.10) into (4.7) yields

$$\mathcal{L}\left[\sum_{n=0}^{\infty} y_n\right] = \Phi(y_\gamma) + \sum_{n=0}^{\infty} A_n. \tag{4.11}$$

From equation (4.11), if we set

$$\mathcal{L}y_0 = \Phi(y_\gamma) \tag{4.12}$$

then

$$\mathcal{L}y_{n+1} = A_n, \qquad n = 0, 1, 2, \ldots \tag{4.13}$$

Equations (4.12) and (4.13) are solved recursively for $y_0, y_1, y_2, \ldots$ subject to the underlying boundary conditions (4.2). The Kth order approximate solution for $y(x)$ is obtained as

$$Y_K = y_0 + y_1 + y_2 + \ldots + y_K \tag{4.14}$$

where $\lim_{K\to\infty} Y_K(x) = y(x)$. The solutions y_K are obtained as solutions of (4.12) and (4.13). For example, when $K = 0$, we obtain

$$y \approx y_0, \tag{4.15}$$

where y_0 is obtained as a solution of

$$\mathcal{L}y_0 = \Phi(y_\gamma). \tag{4.16}$$

This gives the the following iteration scheme

$$\mathcal{L}y_{r+1} = \Phi(y_r), \tag{4.17}$$

which, using equations (4.6) and (4.8) becomes

$$y''_{r+1} + \frac{m}{x}y'_{r+1} + y_{r+1}\frac{\partial f}{\partial y}(y_r) = y_r\frac{\partial f}{\partial y}(y_r) - f(y_r). \tag{4.18}$$

The iteration scheme (4.18) is the standard quasilinearisation method (QLM) scheme that can be used to determine the $(r+1)$th iterative approximation y_{r+1} of the solution of the governing equations (4.1). Evaluating all derivatives of the governing nonlinear function $f(y)$ with respect to y at y_0 instead of y_r in equations (4.16)-(4.18) gives a new iterative scheme

$$y''_{r+1} + \frac{m}{x}y'_{r+1} + y_{r+1}\frac{\partial f}{\partial y}(y_0) = y_r\frac{\partial f}{\partial y}(y_0) - f(y_r). \tag{4.19}$$

The new iterative scheme (4.19) is called the reduced quasilinearization method (RQLM) referred hereafter to as **Scheme 0**. **Scheme 0** can be rewritten in operator form as

$$\mathcal{L}_1 y_{r+1} = \Phi_1(y_r). \tag{4.20}$$

where

$$\begin{aligned} \mathcal{L}_1 y_{r+1} &= y''_{r+1} + \frac{m}{x} y'_{r+1} + y_{r+1} \frac{\partial f}{\partial y}(y_0), \\ \Phi_1(y_r) &= y_r \frac{\partial f}{\partial y}(y_0) - f(y_r). \end{aligned}$$

For $K = 1$, we derive the SADM based higher order QLM of order 1 called **Scheme 1** as follows,

$$y \approx y_0 + y_1, \tag{4.21}$$

Applying (4.13), we obtain y_1 as a solution of

$$\mathcal{L}_1 y_1 = F(y_0). \tag{4.22}$$

This gives rise to the iteration scheme

$$y''_{r+1} + \frac{m}{x} y'_{r+1} + y_{r+1} \frac{\partial f}{\partial y}(y_0) = \Phi_1(y_r) + F(y_{0,r+1}), \tag{4.23}$$

where $F(y_{0,r+1}) = -g(y_{0,r+1})$ and $y_{0,r+1}$ is obtained as the solution of

$$y''_{0,r+1} + \frac{m}{x} y'_{0,r+1} + y_{0,r+1} \frac{\partial f}{\partial y}(y_0) = \Phi_1(y_r). \tag{4.24}$$

Similarly, for $K = 2$ we formulate the 2^{nd} order SADM based QLM named **Scheme 2** as follows

$$y \approx y_0 + y_1 + y_2, \tag{4.25}$$

where y_2 is obtained as a solution of equation (4.13). Therefore, we must solve

$$\mathcal{L}_1 y_2 = y_1 F_y(y_0). \tag{4.26}$$

This produces the 2^{nd} higher order iteration scheme

$$y''_{r+1} + \frac{m}{x}y'_{r+1} + y_{r+1}\frac{\partial f}{\partial y}(y_r) = \Phi_1(y_r) + F(y_{0,r+1}) + y_{1,r+1}F_y(y_{0,r+1}) \quad (4.27)$$

where $y_{1,r+1}$ is the solution of

$$\mathcal{L}_1 y_{1,r+1} = F(y_{0,r+1}) \quad (4.28)$$

The linear operators $\mathcal{L}$ and $\mathcal{L}_1$ can not be solved analytically hence a numerical method is needed to solve the generated iterative schemes. In this work, we shall employ the Chebyshev pseudo spectral method. Under this method the linear operators become easily invertible. The initial approximation $(y_\gamma(x))$ is always chosen such that it satisfies the boundary conditions hence

$$y_\gamma(x) = \frac{B_2}{(e-1)(B_1+1)}[e^x - x]$$

4.1.1 Test for convergence

In this work, we are interested in giving an account about the performance of each iterative schemes based on convergence, rate of convergence and level accuracy of the numerical approximation. In this section we present the procedure used to measure the latter 3 parameters. To test if the method converges we consider the infinite norm(e_i) at each i^{th} iteration. Each scheme is said to converges if

$$e_i = \|y_* - y_i\|_\infty,$$

where y_* is the exact solution and y_i is the approximate solution of $y*$ at the i^{th} iteration. In short, the scheme converges if the infinity norms between successive iterations decreases with increase in the number of iterations i(i.e. $e_1 < e_2 < e_3 < ...$).

A method is said to converge with the rate p if

$$\lim_{i\to\infty} \frac{\|y_{i+1} - y_*\|_\infty}{\|y_i - y_*\|_\infty^p} = K, \tag{4.29}$$

where K is a positive finite constant. Equation (4.29) can be reduced to

$$\frac{e_{i+2}}{e_{i+1}} = \left(\frac{e_{i+1}}{e_i}\right)^p. \tag{4.30}$$

Applying natural logarithm on both sides of (4.30) we get the convergence rate p in explicit form:

$$p = \frac{\ln(e_{i+2}/e_{i+1})}{\ln(e_{i+1}/e_i)}. \tag{4.31}$$

where $e_{i+2},\ e_{i+1},\ e_i$ are infinite norms computed for three consecutive iterations.

Its worth mentioning at this stage that we will test the level of accuracy of the method by considering a simple absolute error between the approximate and exact solutions.

4.2 Test samples

In this section we reveal the equations governing our sampled models. These models have once been solved in literature using numerical and analytical methods.

4.2.1 Example 1

The nonlinear singular second order BVP

$$y''(x) + \frac{2}{x}y'(x) + \lambda e^{-ky(x)} = 0, \quad \lambda > 0. \tag{4.32}$$

subject to the boundary conditions

$$y'(0) = 0, \qquad B_1 y(1) + y'(1) = B_2. \tag{4.33}$$

describes the nonlinear thermal conductivity inside the human head [70, 71, 76]. Here, y is the absolute temperature of the human head and x is the unit radial distance measured from the centre to the periphery of the head. The physical constants λ, k and $B_i,\ i = 1, 2$ represents the thermogenesis heat production parameter, metabolic thermogenesis slope parameter and the Biot number respectively.

4.2.2 Example 2

The nonlinear singular BVP

$$y''(x) + \frac{2}{x}y'(x) - \frac{ny}{y + k_m} = 0, \tag{4.34}$$

subject to the boundary conditions

$$y'(0) = 0, \qquad 5y(1) + y'(1) = 5. \tag{4.35}$$

models the steady-state oxygen diffusion in a spherical cell with Michaelis-Menten uptake Kinetics [86, 87]. The normalized variables y and x represent the oxygen tension and the unit radius of the cell respectively. Here, n and k_m are constants involving the diffusion coefficient, maximum reaction rate , the Michaelis constant K_m and the permeability constant of the cell membrane.

4.2.3 Example 3

Lastly we will solve a singular non linear second order boundary value problem given by:

$$y''(x) + \left(1 + \frac{b}{x}\right) y'(x) - \frac{5x^3(5x^5e^y - x - b - 4)}{4 + x^5} = 0, \tag{4.36}$$

subject to the boundary conditions

$$y'(0) = 0, \qquad y(1) + 5y'(1) = \ln\left(\frac{1}{5}\right) - 5. \tag{4.37}$$

With the exact solution $y(x) = \ln\left(\frac{1}{4+x^5}\right)$.

4.3 Application of the iterative schemes on the test samples

In this section we illustrate the application of the outlined QLM and SADM based higher order RQLM on the test models presented earlier on.

4.3.1 Solution to Example 1 by QLM

Here, the QLM iterative scheme (4.18) is employed as a method of solution to equation (4.32) that models the thermal conductivity in the human head. From the model, we first identify the governing nonlinear term as

$$f(y) = \lambda e^{-ky}. \tag{4.38}$$

It follows that

$$\frac{\partial f}{\partial y}(y) = -\lambda k e^{-ky}. \tag{4.39}$$

Substituting equations (4.38) and (4.39) into the QLM iterative scheme (4.18) we obtain

$$y''_{r+1} + \frac{2}{x}y'_{r+1} - y_{r+1}\left(\lambda k e^{-ky_r}\right) = \Phi(y_r), \tag{4.40}$$

where

$$\Phi(y_r) = -y_r\left(\lambda k e^{-ky_r}\right) - \lambda e^{-ky_r}.$$

Applying the pseudo Spectral collocation method to solve the resultant linear iterative scheme (4.40), we get

$$\mathcal{L}y_{r+1} = \Phi(y_r) \tag{4.41}$$

subject to the following boundary conditions

$$y'_{r+1}(0) = 0, \qquad B_1 y_{r+1}(1) + y'_{r+1}(1) = B_2. \tag{4.42}$$

Here,

$$\mathcal{L} = \mathbf{D}^2 + \frac{2}{x}\mathbf{D} - diag\left(\lambda k e^{-ky_r}\right).$$

4.3.2 Solution to Example 1 by Scheme-0, Scheme-1 and Scheme-2

Under this section, we present the solution to the thermal conductivity in the human head problem (4.32) by the new RQLM (Scheme-0) and its SADM based higher order schemes, Scheme-1 and Scheme 2. Under these schemes,

$$\frac{\partial f}{\partial y}(y_r) = -\lambda k e^{-ky_0}. \tag{4.43}$$

- **Scheme 0**

  In terms of the RQLM iterative scheme (4.19), the solution to (4.32) is given as

  $$y''_{r+1} + \frac{2}{x}y'_{r+1} - y_{r+1}\left(\lambda k e^{-ky_0}\right) = \Phi(y_r), \tag{4.44}$$

  where

  $$\Phi(y_r) = -y_r\left(\lambda k e^{-ky_0}\right) - \lambda e^{-ky_r}.$$

  Applying the pseudo Spectral collocation method to solve the resultant linear iterative scheme (4.44), we get

  $$\mathcal{L}y_{r+1} = \Phi(y_r) \tag{4.45}$$

  subject to the following boundary conditions

  $$y'_{r+1}(0) = 0, \qquad B_1 y_{r+1}(1) + y'_{r+1}(1) = B_2. \tag{4.46}$$

  Here,

  $$\mathcal{L} = \mathbf{D}^2 + \frac{2}{x}\mathbf{D} - diag\left(\lambda k e^{-ky_0}\right).$$

- **Scheme 1**

  According to Scheme-1 iterative scheme (4.23)-(4.24), the solution to

the governing equation (4.32) is given as

$$y''_{r+1} + \frac{2}{x}y'_{r+1} + y_{r+1}\left(-\lambda k e^{-ky_0}\right) = y_r\left(-\lambda k e^{-ky_0}\right) - \lambda e^{-ky_r} + F(y_{0,r+1}), \tag{4.47}$$

where

$$F(y_{0,r+1}) = -\left[\lambda e^{-ky_{0,r+1}} - \lambda e^{-ky_{r+}} - (y_{0,r+1} - y_r)\left(-\lambda k e^{-ky_0}\right)\right].$$

We solve

$$y''_{0,r+1} + \frac{2}{x}y'_{0,r+1} + y_{0,r+1}\left(-\lambda k e^{-ky_0}\right) = y_r\left(-\lambda k e^{-ky_0}\right) - \lambda e^{-ky_r}. \tag{4.48}$$

to get $y_{0,r+1}$.

Applying the pseudo spectral method to solve the iterative schemes (4.47) and (4.48), we get

$$\mathcal{L}_1 y_{r+1} = C_1, \tag{4.49}$$

subject to

$$y'_{r+1}(0) = 0, \qquad B_1 y_{r+1}(1) + y'_{r+1}(1) = 0 \tag{4.50}$$

and

$$\mathcal{L}_1 y_{0,r+1} = C_2, \tag{4.51}$$

subject to

$$y'_{0,r+1}(0) = 0, \qquad B_1 y_{0,r+1}(1) + y'_{r+1}(1) = B_2. \tag{4.52}$$

Here,

$$\begin{aligned} \mathcal{L}_1 &= \mathbf{D}^2 + \frac{2}{x}\mathbf{D} + diag\left(-\lambda k e^{-ky_0}\right), \\ C_1 &= y_r\left(-\lambda k e^{-ky_0}\right) - \lambda e^{-ky_r} + F(y_{0,r+1}), \\ C_2 &= y_r\left(-\lambda k e^{-ky_0}\right) - \lambda e^{-ky_r}. \end{aligned}$$

We remark that C_1 and C_2 are column vectors of the equivalent functions, evaluated at the collocation points.

- **Scheme 2**

  The Scheme-2 iterative scheme (4.27)-(4.28), the solution to the governing equation (4.32) is given as

$$\begin{aligned} y''_{r+1} + \frac{2}{x}y'_{r+1} + y_{r+1}\left(-\lambda k e^{-ky_0}\right) &= -y_r\left(\lambda k e^{-ky_0}\right) + \lambda e^{-ky_r} + F(y_{0,r+1}) \\ &\quad + y_{1,r+1}F_y(y_{0,r+1}), \end{aligned} \tag{4.53}$$

  where

$$\begin{aligned} F(y_{0,r+1}) &= -\left[\lambda e^{-ky_{0,r+1}} - \lambda e^{-ky_{r+}} - (y_{0,r+1} - y_r)\left(-\lambda k e^{-ky_0}\right)\right], \\ F_y(y_{0,r+1}) &= -\left(-\lambda k e^{-ky_{0,r+1}} + \lambda k e^{-ky_0}\right). \end{aligned}$$

  The component $y_{1,r+1}$ is the solution of

$$y''_{1,r+1} + \frac{2}{x}y'_{1,r+1} + y_{1,r+1}\left(-\lambda k e^{-ky_0}\right) = F(y_{0,r+1}), \tag{4.54}$$

  and $y_{0,r+1}$ is the solution of

$$y''_{0,r+1} + \frac{2}{x}y'_{0,r+1} + y_{0,r+1}\left(-\lambda k e^{-ky_0}\right) = y_r\left(-\lambda k e^{-ky_0}\right) - \lambda e^{-ky_r}. \tag{4.55}$$

  Applying the pseudo Spectral method to solve the 2^{nd} order iterative scheme (4.53)-(4.55), we get

$$\mathcal{L}_1 y_{r+1} = C_1, \tag{4.56}$$

  subject to

$$y'_{r+1}(0) = 0, \qquad B_1 y_{r+1}(1) + y'_{r+1}(1) = 0, \tag{4.57}$$

$$\mathcal{L}_1 y_{1,r+1} = C_2, \tag{4.58}$$

subject to

$$y'_{r+1}(0) = 0, \qquad B_1 y_{r+1}(1) + y'_{r+1}(1) = 0, \tag{4.59}$$

$$\mathcal{L}_1 y_{0,r+1} = C_3, \tag{4.60}$$

subject to

$$y'_{0,r+1}(0) = 0, \qquad B_1 y_{0,r+1}(1) + y'_{r+1}(1) = B_2, \tag{4.61}$$

respectively.

Here,

$$\begin{aligned}
\mathcal{L}_1 &= \mathbf{D}^2 + \frac{2}{x}\mathbf{D} + diag\left(-\lambda k e^{-k y_0}\right), \\
C_1 &= y_r\left(-\lambda k e^{-k y_0}\right) - \lambda e^{-k y_r} + F(y_{0,r+1}) + y_{1,r+1} F_y(y_{0,r+1}), \\
C_2 &= F(y_{0,r+1}), \\
C_3 &= y_r\left(-\lambda k e^{-k y_0}\right) - \lambda e^{-k y_r}.
\end{aligned}$$

We remark that C_1, C_2, C_3 are column vectors of the equivalent functions, evaluated at the collocation points.

4.3.3 Solution to Example 2 by QLM

Here, we present the treatment of the oxygen diffusion model (4.34) using the QLM iterative scheme (4.18). From the model, we first identify the governing nonlinear term as

$$f(y) = -\frac{ny}{y + k_m}. \tag{4.62}$$

From (4.62),

$$\frac{\partial f}{\partial y}(y) = -\frac{n k_m}{(y + k_m)^2}. \tag{4.63}$$

Substituting equations (4.62) and (4.63) into the QLM iterative scheme (4.18) we obtain

$$y''_{r+1} + \frac{2}{x}y'_{r+1} - y_{r+1}\left(\frac{nk_m}{(y_r + k_m)^2}\right) = \Phi(y_r), \tag{4.64}$$

where

$$\Phi(y_r) = -y_r\left(\frac{nk_m}{(y_r + k_m)^2}\right) + \frac{ny_r}{y_r + k_m}.$$

We then solve the resultant linear iterative scheme (4.64) using the pseudo Spectral collocation method as follows

$$\mathcal{L}y_{r+1} = \Phi(y_r) \tag{4.65}$$

subject to the following boundary conditions

$$y'_{r+1}(0) = 0, \quad 5y_{r+1}(1) + y'_{r+1}(1) = 5. \tag{4.66}$$

Here,

$$\mathcal{L} = \mathbf{D}^2 + \frac{2}{x}\mathbf{D} - diag\left(\frac{nk_m}{(y_r + k_m)^2}\right).$$

4.3.4 Solution to Example 2 by Schem-0, Scheme-1 and Scheme-2

Under this section, we present the solution to the oxygen diffusion model (4.34) by the new RQLM (Scheme-0) and its SADM based higher order schemes, Scheme-1 and Scheme-2. Under these schemes,

$$\frac{\partial f}{\partial y}(y_r) = -\frac{nk_m}{(y_0 + k_m)^2}. \tag{4.67}$$

- **Scheme 0**

  In terms of the RQLM iterative scheme (4.19), the solution to (4.34) is given as

$$y''_{r+1} + \frac{2}{x}y'_{r+1} - y_{r+1}\left(\frac{nk_m}{(y_0 + k_m)^2}\right) = \Phi(y_r), \tag{4.68}$$

where

$$\Phi(y_r) = -y_r\left(\frac{nk_m}{(y_0+k_m)^2}\right) + \frac{ny_r}{y_r+k_m}.$$

Applying the pseudo Spectral collocation method to solve the resultant linear iterative scheme (4.68), we get

$$\mathcal{L}y_{r+1} = \Phi(y_r) \tag{4.69}$$

subject to the following boundary conditions

$$y'_{r+1}(0) = 0, \qquad 5y_{r+1}(1) + y'_{r+1}(1) = 5. \tag{4.70}$$

Here,

$$\mathcal{L} = \mathbf{D}^2 + \frac{2}{x}\mathbf{D} - diag\left(\frac{nk_m}{(y_0+k_m)^2}\right).$$

- **Scheme 1**

  According to Scheme-1 iterative scheme (4.23)-(4.24), the solution to the governing equation (4.34) is given as

$$\begin{aligned} y''_{r+1} + \frac{2}{x}y'_{r+1} + y_{r+1}\left(-\frac{nk_m}{(y_0+k_m)^2}\right) &= y_r\left(-\frac{nk_m}{(y_0+k_m)^2}\right) + \frac{ny_r}{y_r+k_m} \\ &\quad + F(y_{0,r+1}), \end{aligned} \tag{4.71}$$

  where

$$F(y_{0,r+1}) = -\left[-\frac{ny_{0,r+1}}{y_{0,r+1}+k_m} + \frac{ny_r}{y_r+k_m} + (y_{0,r+1}-y_r)\left(\frac{nk_m}{(y_0+k_m)^2}\right)\right].$$

  We solve

$$y''_{0,r+1} + \frac{2}{x}y'_{0,r+1} - y_{0,r+1}\left(\frac{nk_m}{(y_0+k_m)^2}\right) = y_r\left(-\frac{nk_m}{(y_0+k_m)^2}\right) + \frac{ny_r}{y_r+k_m}. \tag{4.72}$$

  to get $y_{0,r+1}$.

Applying the pseudo Spectral method to solve the iterative schemes (4.71) and (4.72), we get

$$\mathcal{L}_1 y_{r+1} = C_1, \tag{4.73}$$

subject to

$$y'_{r+1}(0) = 0, \qquad 5y_{r+1}(1) + y'_{r+1}(1) = 0 \tag{4.74}$$

and

$$\mathcal{L}_1 y_{0,r+1} = C_2, \tag{4.75}$$

subject to

$$y'_{0,r+1}(0) = 0, \qquad 5y_{0,r+1}(1) + y'_{r+1}(1) = 5, \tag{4.76}$$

respectively.

Here,

$$\begin{aligned}
\mathcal{L}_1 &= \mathbf{D}^2 + \frac{2}{x}\mathbf{D} + diag\left(-\lambda k e^{-ky_0}\right), \\
C_1 &= y_r\left(-\frac{nk_m}{(y_0+k_m)^2}\right) + \frac{ny_r}{y_r+k_m} + F(y_{0,r+1}), \\
C_2 &= y_r\left(-\frac{nk_m}{(y_0+k_m)^2}\right) + \frac{ny_r}{y_r+k_m}.
\end{aligned}$$

We remark that C_1 and C_2 are column vectors of the equivalent functions, evaluated at the collocation points.

- **Scheme 2**

  According to Scheme-2 iterative scheme (4.27)-(4.28), the solution to the governing equation (4.34) is given as

$$\begin{aligned}
y''_{r+1} + \frac{2}{x}y'_{r+1} - y_{r+1}\left(\frac{nk_m}{(y_0+k_m)^2}\right) &= y_r\left(-\frac{nk_m}{(y_0+k_m)^2}\right) + \frac{ny_r}{y_r+k_m} \\
&\quad + F(y_{0,r+1}) \\
&\quad + y_{1,r+1}F_y(y_{0,r+1}),
\end{aligned} \tag{4.77}$$

where

$$\begin{aligned} F(y_{0,r+1}) &= \left[\frac{ny_{0,r+1}}{y_{0,r+1}+k_m} - \frac{ny_r}{y_r+k_m} - (y_{0,r+1}-y_r)\left(\frac{nk_m}{(y_0+k_m)^2}\right)\right]. \\ F_y(y_{0,r+1}) &= \left(\frac{nk_m}{(y_{0,r+1}+k_m)^2} - \frac{nk_m}{(y_0+k_m)^2}\right) \end{aligned}$$

The unknown, $y_{1,r+1}$ is the solution of

$$y''_{1,r+1} + \frac{2}{x}y'_{1,r+1} + y_{1,r+1}\left(-\frac{nk_m}{(y_0+k_m)^2}\right) = F(y_{0,r+1}), \tag{4.78}$$

and $y_{0,r+1}$ is the solution of

$$\begin{aligned} y''_{0,r+1} + \frac{2}{x}y'_{0,r+1} - y_{0,r+1}\left(\frac{nk_m}{(y_0+k_m)^2}\right) &= y_r\left(-\frac{nk_m}{(y_0+k_m)^2}\right) \\ &\quad + \frac{ny_r}{y_r+k_m}. \end{aligned} \tag{4.79}$$

Applying the pseudo spectral method to solve the 2^{nd} order iterative scheme (4.77)-(4.79), we get

$$\mathcal{L}_1 y_{r+1} = C_1, \tag{4.80}$$

subject to

$$y'_{r+1}(0) = 0, \qquad 5y_{r+1}(1) + y'_{r+1}(1) = 0, \tag{4.81}$$

$$\mathcal{L}_1 y_{1,r+1} = C_2, \tag{4.82}$$

subject to

$$y'_{r+1}(0) = 0, \qquad 5y_{r+1}(1) + y'_{r+1}(1) = 0, \tag{4.83}$$

and

$$\mathcal{L}_1 y_{0,r+1} = C_3, \tag{4.84}$$

subject to

$$y'_{0,r+1}(0) = 0, \qquad 5y_{0,r+1}(1) + y'_{r+1}(1) = 5, \tag{4.85}$$

respectively.

Here,

$$\begin{aligned}
\mathcal{L}_1 &= \mathbf{D}^2 + \frac{2}{x}\mathbf{D} - diag\left(\frac{nk_m}{(y_0+k_m)^2}\right), \\
C_1 &= -y_r\left(\frac{nk_m}{(y_0+k_m)^2}\right) + \frac{ny_r}{y_r+k_m} + F(y_{0,r+1}) + y_{1,r+1}F_y(y_{0,r+1}), \\
C_2 &= F(y_{0,r+1}), \\
C_3 &= -y_r\left(\frac{nk_m}{(y_0+k_m)^2}\right) + \frac{ny_r}{y_r+k_m}.
\end{aligned}$$

We remark that C_1, C_2 and C_3 are column vectors of the equivalent functions, evaluated at the collocation points.

4.3.5 Solution to Example 3 by QLM

In this section, we show how the QLM iterative scheme (4.18) is used to solve Example 3 of our test samples. The governing nonlinear function in equation (4.36) is

$$f(y) = -\frac{25x^8e^y}{4+x^5}. \tag{4.86}$$

From (4.62),

$$\frac{\partial f}{\partial y}(y) = -\frac{25x^8e^y}{4+x^5}. \tag{4.87}$$

According to the QLM iterative scheme (4.18), the solution to equation (4.36) is given by

$$y''_{r+1} + \frac{2}{x}y'_{r+1} - y_{r+1}\left(\frac{25x^8e^{y_r}}{4+x^5}\right) = \Phi(y_r), \tag{4.88}$$

where

$$\Phi(y_r) = -y_r\left(\frac{25x^8e^{y_r}}{4+x^5}\right) + \frac{5x^3(5x^5e^{y_r} - x - b - 4)}{4+x^5}.$$

We then solve the resultant linear iterative scheme (4.88) using the pseudo Spectral collocation method , as follows

$$\mathcal{L}y_{r+1} = \Phi(y_r) \tag{4.89}$$

subject to the following boundary conditions

$$y'_{r+1}(0) = 0, \quad y(1) + 5y'_{r+1}(1) = \ln\left(\frac{1}{5}\right) - 5. \tag{4.90}$$

Here,

$$\mathcal{L} = \mathbf{D}^2 + \frac{2}{x}\mathbf{D} - diag\left(\frac{25x^8 e^{y_r}}{4+x^5}\right).$$

4.3.6 Solution to Example 3 by Scheme-0, Scheme-1 and Scheme-2

Under this section, we present the solution to Example 3 in (4.36) by the new RQLM (Scheme-0) and its SADM based higher order schemes, Scheme-1 and Scheme 2. Under these schemes,

$$\frac{\partial f}{\partial y}(y_r) = -\frac{25x^8 e^{y_0}}{4+x^5}. \tag{4.91}$$

- **Scheme 0**

  In terms of the RQLM iterative scheme (4.19), the solution to (4.36) is given as

  $$y''_{r+1} + \frac{2}{x}y'_{r+1} - y_{r+1}\left(\frac{25x^8 e^{y_0}}{4+x^5}\right) = \Phi(y_r), \tag{4.92}$$

  where

  $$\Phi(y_r) = -y_r\left(\frac{25x^8 e^{y_0}}{4+x^5}\right) + \frac{5x^3(5x^5 e^{y_r} - x - b - 4)}{4+x^5}.$$

  Applying the pseudo Spectral collocation method to solve the resultant linear iterative scheme (4.92), we get

  $$\mathcal{L}y_{r+1} = \Phi(y_r) \tag{4.93}$$

  subject to the following boundary conditions

  $$y'_{r+1}(0) = 0, \quad y(1) + 5y'_{r+1}(1) = \ln\left(\frac{1}{5}\right) - 5. \tag{4.94}$$

Here,

$$\mathcal{L} = \mathbf{D}^2 + \frac{2}{x}\mathbf{D} - diag\left(\frac{25x^8 e^{y_0}}{4+x^5}\right).$$

- **Scheme 1**

  According to Scheme-1 iterative scheme (4.23)-(4.24), the solution to the governing equation (4.36) is given as

$$\begin{aligned} y''_{r+1} + \frac{2}{x}y'_{r+1} + y_{r+1}\left(-\frac{25x^8 e^{y_0}}{4+x^5}\right) &= \frac{5x^3(5x^5 e^{y_r} - x - b - 4)}{4+x^5} \\ &\quad + F(y_{0,r+1}) \\ &\quad - y_r\left(\frac{25x^8 e^{y_0}}{4+x^5}\right), \end{aligned} \tag{4.95}$$

  where

$$F(y_{0,r+1}) = \left[\frac{25x^8 e^{y_{0,r+1}}}{4+x^5} - \frac{25x^8 e^{y_r}}{4+x^5} + (y_{0,r+1} - y_r)\left(\frac{25x^8 e^{y_0}}{4+x^5}\right)\right].$$

  The solution to

$$\begin{aligned} y''_{0,r+1} + \frac{2}{x}y'_{0,r+1} - y_{0,r+1}\left(\frac{25x^8 e^{y_0}}{4+x^5}\right) &= \frac{5x^3(5x^5 e^{y_r} - x - b - 4)}{4+x^5} \\ &\quad - y_r\left(\frac{25x^8 e^{y_0}}{4+x^5}\right). \end{aligned} \tag{4.96}$$

  gives $y_{0,r+1}$.

  Applying the pseudo spectral method to solve the iterative schemes (4.95) and (4.96), we get

$$\mathcal{L}_1 y_{r+1} = C_1, \tag{4.97}$$

  subject to

$$y'_{r+1}(0) = 0, \quad y(1) + 5y'_{r+1}(1) = 0. \tag{4.98}$$

  and

$$\mathcal{L}_1 y_{0,r+1} = C_2, \tag{4.99}$$

subject to

$$y'_{0,r+1}(0) = 0, \quad y(1) + 5y'_{0,r+1}(1) = \ln\left(\frac{1}{5}\right) - 5. \tag{4.100}$$

Here,

$$\begin{aligned}
\mathcal{L}_1 &= \mathbf{D}^2 + \frac{2}{x}\mathbf{D} + diag\left(-\lambda k e^{-ky_0}\right), \\
C_1 &= -y_r\left(\frac{25x^8e^{y_0}}{4+x^5}\right) + \frac{5x^3(5x^5e^{y_r} - x - b - 4)}{4+x^5} + F(y_{0,r+1}), \\
C_2 &= -y_r\left(\frac{25x^8e^{y_0}}{4+x^5}\right) + \frac{5x^3(5x^5e^{y_r} - x - b - 4)}{4+x^5}.
\end{aligned}$$

We remark that C_1 and C_2 are column vectors of the equivalent functions, evaluated at the collocation points.

- **Scheme 2**

  According to the Scheme-2 iterative scheme (4.27)-(4.28), the solution to the governing equation (4.36) is given as

$$\begin{aligned}
y''_{r+1} + \frac{2}{x}y'_{r+1} - y_{r+1}\left(\frac{25x^8e^{y_0}}{4+x^5}\right) &= \frac{5x^3(5x^5e^{y_r} - x - b - 4)}{4+x^5} \\
&\quad + F(y_{0,r+1}) + y_{1,r+1}F_y(y_{0,r+1}) \\
&\quad - y_r\left(\frac{25x^8e^{y_0}}{4+x^5}\right),
\end{aligned} \tag{4.101}$$

  where

$$\begin{aligned}
F(y_{0,r+1}) &= \left[\frac{25x^8e^{y_{0,r+1}}}{4+x^5} + \frac{25x^8e^{y_r}}{4+x^5} - (y_{0,r+1} - y_r)\left(\frac{25x^8e^{y_0}}{4+x^5}\right)\right]. \\
F_y(y_{0,r+1}) &= \left(\frac{25x^8e^{y_{0,r+1}}}{4+x^5} - \frac{25x^8e^{y_0}}{4+x^5}\right)
\end{aligned}$$

  The unknown function, $y_{1,r+1}$ is the solution of

$$y''_{r+1} + \frac{2}{x}y'_{r+1} - y_{r+1}\left(\frac{25x^8e^{y_0}}{4+x^5}\right) = F_y(y_{0,r+1}), \tag{4.102}$$

  and $y_{0,r+1}$ is the solution of

$$y''_{0,r+1} + \frac{2}{x}y'_{0,r+1} - y_{0,r+1}\left(\frac{25x^8e^{y_0}}{4+x^5}\right) = \frac{5x^3(5x^5e^{y_r} - x - b - 4)}{4+x^5} - y_r\left(\frac{25x^8e^{y_0}}{4+x^5}\right). \quad (4.103)$$

Employing the pseudo spectral method to solve the iterative schemes (4.101) and (4.103), we get

$$\mathcal{L}_1 y_{r+1} = C_1, \quad (4.104)$$

subject to

$$y'_{r+1}(0) = 0, \quad y(1) + 5y'_{r+1}(1) = 0, \quad (4.105)$$

$$\mathcal{L}_1 y_{1,r+1} = C_2, \quad (4.106)$$

subject to

$$y'_{r+1}(0) = 0, \quad y(1) + 5y'_{r+1}(1) = 0. \quad (4.107)$$

and

$$\mathcal{L}_1 y_{0,r+1} = C_3, \quad (4.108)$$

subject to

$$y'_{0,r+1}(0) = 0, \quad y(1) + 5y'_{0,r+1}(1) = \ln\left(\frac{1}{5}\right) - 5. \quad (4.109)$$

Here,

$$\begin{aligned}
\mathcal{L}_1 &= \mathbf{D}^2 + \frac{2}{x}\mathbf{D} + diag\left(-\lambda k e^{-ky_0}\right), \\
C_1 &= -y_r\left(\frac{25x^8e^{y_0}}{4+x^5}\right) + \frac{5x^3(5x^5e^{y_r} - x - b - 4)}{4+x^5} \\
&\quad + F(y_{0,r+1}) + y_{1,r+1}F_y(y_{0,r+1}), \\
C_2 &= F(y_{0,r+1}), \\
C_3 &= -y_r\left(\frac{25x^8e^{y_0}}{4+x^5}\right) + \frac{5x^3(5x^5e^{y_r} - x - b - 4)}{4+x^5}.
\end{aligned}$$

We remark that C_1, C_2 and C_3 are column vectors of the equivalent functions, evaluated at the collocation points.

4.4 Presentation and discussion of results

We present the approximate solutions to the three sampled models by the four iterative schemes discussed earlier on. These methods are the QLM, **Scheme 0**,**Scheme 1** and **Scheme 2**. This is aimed at comparing the effectiveness and performance amongst the schemes in solving the singular nonlinear two point BVPs arising in physiology. The results are validated against `bvp4c`, the literature results and exact solution where applicable.

Table 4.1 shows the number of iterations and CPU time in seconds taken by the respective iterative schemes to converge to within 14 decimal digits accuracy to the solution of $y(0)$ for Example 1. Each method used 20 collocation points to reach this level of accuracy and the values of the governing constants used are, $k = \lambda = B_1 = B_2 = 1$.

Table 4.1: The approximate solution of $y(0)$ for Example 1 by the **Schemes** when $k = \lambda = B_1 = B_2 = 1$, $N = 20$.

iter.	**Scheme 0**	**Scheme 1**	**Scheme 2**	QLM
2	1.15415343396382	1.16073569167800	1.16081858865205	1.16065213228202
4	1.16073569167800	1.16081980617450	1.16081981958758	1.16081981959005
5	1.16081036571601	1.16081981942064	1.16081981959005	1.16081981959005
6	1.16081875721789	1.16081981958791	1.16081981959005	1.16081981959005
8	1.16081980617450	1.16081981959005	1.16081981959005	1.16081981959005
10	1.16081981942064	1.16081981959005	1.16081981959005	1.16081981959005
12	1.16081981958791	1.16081981959005	1.16081981959005	1.16081981959005
14	1.16081981959003	1.16081981959005	1.16081981959005	1.16081981959005
15	1.16081981959005	1.16081981959005	1.16081981959005	1.16081981959005
16	1.16081981959005	1.16081981959005	1.16081981959005	1.16081981959005
Time(s)	0.187	0.047	0.031	0.062
Other methods	$y(0)$			
`bvp4c`	1.16081981959005			
ADM [76]	1.16081981959015			
SLM [70]	1.16081981959015			

From Table 4.1, **Scheme 2** took 5 iterations which is roughly half of the 8 iterations taken by **Scheme 1** which is in turn almost half of the 15 iterations taken by **Scheme 0** to converge to the approximate solution within 10^{-14}. The QLM took the least number of iterations to converge to the same level of accuracy. It is worth noting that increasing the order of the schemes by one reduces the number of iterations by almost half. Furthermore, in terms of the CPU time, **Scheme 2** is the fastest with $0.031s$ followed by **Scheme 1** with $0.047s$ and then the QLM with just $0.062s$. **Scheme 0** is the slowest. This suggest that **Scheme 1** and **Scheme 2** are more efficient than the QLM and **Scheme 0** in terms of computation time. The table also shows that the approximate solutions by each iterative scheme are in excellent agreement with `bvp4c` results and the literature results by SLM in [70] and ADM in [76].

Table 4.2 shows the same comparison as in Table 4.1 but for different values of the governing parameters. In Table 4.2, $k = \lambda = 1$, $B_1 = 0.1$ and $B_2 = 0$.

Table 4.2: The approximate solution of $y(0)$ for Example 1 by the **Schemes** when $k = \lambda = 1,\ B_1 = 0.1,\ B_2 = 0,\ N = 100$

	Scheme 0	**Scheme 1**	**Scheme 2**
5	1.12539419496037	1.14622914819406	1.14700621185592
10	1.14622914819406	1.14703786239255	1.14703901755740
15	1.14698009671963	1.14703901320120	1.14703901932914
17	1.14703076292017	1.14703901920949	1.14703901932982
20	1.14703786239255	1.14703901932746	1.14703901932982
25	1.14703897559342	1.14703901932982	1.14703901932982
30	1.14703901888377	1.14703901932982	1.14703901932982
35	1.14703901929736	1.14703901932982	1.14703901932982
40	1.14703901932746	1.14703901932982	1.14703901932982
45	1.14703901932965	1.14703901932982	1.14703901932982
49	1.14703901932982	1.14703901932982	1.14703901932982
50	1.14703901932982	1.14703901932982	1.14703901932982
time(s)	6.022	1.279	1.232

Other methods	$y(0)$
`bvp4c`	1.14703901932982
Ref. [70]	1.1470390193298
Ref. [71]	1.14703993670271
Ref. [74]	0.11470486854

All the schemes proved to be reliable since their results are still in excellent agreement with those of `bvp4c` and the SLM in [70] regardless of varying B_1 and B_2. The results by the schemes are much better in terms of accuracy than the third-degree B-spline in [71] and the non-polynomial cubic splines in [74]. The higher order **Scheme 0, 1, 2** matched the `bvp4c` solution by at least 14 decimals. In terms of the number of iterations, the **Scheme 2** is the most efficient with only 17 iterations followed by **Scheme 1** with 17 iterations. **Scheme 0** used the highest number of iterations with 49. When it comes to the CPU time utilised, **Scheme 2** is the fastest followed by **Scheme 1** and lastly **Scheme 0**.

Table 4.3 shows the number of iterations and CPU time in seconds taken by the respective iterative schemes to converge within at least 14 decimal digits accuracy to the solution of $y(0)$ for Example 2. Each iterative scheme used 20 collocation points to reach this level of accuracy and the values of the governing constants were set to be $n = 0.76129$ and $k = 0.03119$.

Table 4.3: The approximate solution of $y(0)$ for Example 2 by the **Schemes** when $n = 0.76129,\ k = 0.03119,\ N = 20$.

iter.	**Scheme 0**	**Scheme 1**	**Scheme 2**	QLM
1	0.82712772931487	0.82847612713825	0.82848324819381	0.82712772931487
2	0.82847612713825	0.82848329017763	0.82848329035968	0.82848328440170
3	0.82848325406224	0.82848329035968	0.82848329035969	0.82848329035971
4	0.82848329017763	0.82848329035969	0.82848329035969	0.82848329035966
5	0.82848329035878	0.82848329035969	0.82848329035969	0.82848329035962
6	0.82848329035968	0.82848329035969	0.82848329035969	0.82848329035962
7	0.82848329035969	0.82848329035969	0.82848329035969	0.82848329035969
8	0.82848329035969	0.82848329035969	0.82848329035969	0.82848329035969
Time(s)	0.031	0.016	0.016	0.018
	`bvp4c`	0.82848329035969		

Scheme 2 took 3 iterations while **Scheme 1** took 4 iterations followed by **Scheme 0** with 7 iterations to converge to at least 14 decimal places. This time around the QLM used the same number of iterations as **Scheme 0**. As in Table 4.2 and 4.1, we see that increasing the order of schemes reduces the number of iterations taken to converge to the correct solution. We can also deduce that the approximate solutions by each iterative scheme are in excellent agreement with `bvp4c` results. In terms of computational time, **Scheme 1** and **Scheme 2** are the most efficient methods followed by the QLM and then **Scheme 0**.

Table 4.4 is an extension of Table 4.3 in the sense that it gives the approximate solution of $y(x)$ for Example 2 instead of the solution of $y(0)$ only. Corresponding to the approximate solutions by each iterative scheme is the maximum absolute error computed against `bvp4c` results.

Table 4.4: The approximate solution of $y(x)$ for Example 2 when $n = 0.76129,\ k = 0.03119,\ N = 100$.

	Scheme 0	**Scheme 1**	**Scheme 2**
x	$y(x)$	$y(x)$	$y(x)$
1.0	0.95094579849648	0.95094579849648	0.95094579849648
0.8	0.90681854806680	0.90681854806680	0.90681854806680
0.6	0.87252831995814	0.87252831995814	0.87252831995814
0.4	0.84805278499588	0.84805278499588	0.84805278499588
0.2	0.83337473359099	0.83337473359099	0.83337473359099
0.0	0.82848329035969	0.82848329035969	0.82848329035969
Norms:	1.774×10^{-13}	1.772×10^{-13}	1.772×10^{-13}
	`bvp4c`	QLM	B-spline [71]
x	$y(x)$	$y(x)$	$y(x)$
1	0.95094579849648	0.95094579849641	0.9509457946
0.8	0.90681854806680	0.90681854783431	0.9068185402
0.6	0.87252831995829	0.87252831796751	0.8725283084
0.4	0.84805278499606	0.84805278245938	0.8480527703
0.2	0.83337473359099	0.83337473311752	0.8333747169
0	0.82848329035969	0.82848329035962	0.8284832729
Norms:		2.537×10^{-9}	1.74×10^{-8}

From Table 4.4, the maximum absolute error by **Scheme 0**, **Scheme 1** and **Scheme 2** is 1.774×10^{-13}, 1.772×10^{-13} and 1.772×10^{-13} respectively. On the other hand, the maximum absolute error by QLM is 2.537×10^{-9} which shows that the latter schemes are more accurate than the QLM by at least 4 decimal places. The third-degree B-spline results in literature have an absolute maximum error of 1.74×10^{-8} which is at least 5 decimals poorer than the higher order schemes.

Table 4.5 shows the number of iterations taken by **Scheme 0** and **Scheme 1** to converge to the solution of $y(0)$ for different values of b in Example 3. Corresponding to each number of iterations is the absolute error with respect to the exact solution. This table also captures the convergence rates of the respective iterative schemes at each iteration for the various b. We remark that Table 4.6 is an extension of Table 4.5. It shows exactly the same information as Table 4.5 but for **Scheme 2** and the QLM.

Table 4.5: The approximate solution of $y(0)$ to Example 3 for varying b by **Scheme 0, 1** compared against the exact solution -1.38629436111989

iter.	$b = 0.25$	$b = 1$	$b = 2$
	Scheme 0		
7	-1.38629049932523	-1.38629153517649	-1.38629245838053
14	-1.38629436106585	-1.38629436109093	-1.38629436110676
21	-1.38629436111989	-1.38629436111989	-1.38629436111989
	Corresponding absolute errors		
7	0.000003861794662	0.000002825943400	0.000001902739358
14	0.000000000054043	0.000000000028956	0.000000000013133
21	0.000000000000000	0.000000000000000	0.000000000000000
	Corresponding convergence rate		
7	0.99997	0.99997	0.99998
14	1.00000	1.00000	1.00000
21	1.00000	1.00000	1.00000
	Scheme 1		
4	-1.38629357885763	-1.38629381361463	-1.38629401271058
8	-1.38629436111767	-1.38629436111880	-1.38629436111945
11	-1.38629436111989	-1.38629436111989	-1.38629436111989
	Corresponding absolute errors		
4	0.000000782262257	0.000000547505257	0.000000348409313
8	0.000000000002218	0.000000000001087	0.000000000000440
11	0.000000000000000	0.000000000000000	0.000000000000000
	Corresponding convergence Rate		
4	1.00000	1.00000	1.00000
8	1.00000	1.00000	1.00000
11	1.00000	1.00000	1.00000

Table 4.6: The approximate solution of $y(0)$ for Example 3.3 for varying b by **Scheme 2** and the QLM compared against the exact solution -1.38629436111989

iter.	$b = 0.25$	$b = 1$	$b = 2$
	Scheme 2		
3	-1.38629417909761	-1.38629423903599	-1.38629428752164
6	-1.38629436111979	-1.38629436111984	-1.38629436111987
7	-1.38629436111989	-1.38629436111989	-1.38629436111989
	Corresponding absolute errors		
3	0.00000018202228	0.00000012208390	0.00000007359825
6	0.00000000000010	0.00000000000005	0.00000000000002
7	0.00000000000000	0.00000000000000	0.00000000000000
	Corresponding convergence rate		
3	0.9998	0.9998	0.9999
6	1.0000	1.0000	1.0000
7	1.0000	1.0000	1.0000
	QLM		
2	-1.38565657865832	-1.38574403014326	-1.38583729717809
3	-1.38629428764471	-1.38629430916682	-1.38629432754799
4	-1.38629436111989	-1.38629436111989	-1.38629436111989
	Corresponding absolute errors		
2	0.000637782461574	0.000550330976634	0.000457063941803
3	0.000000073475185	0.000000051953069	0.000000033571899
4	0.000000000000000	0.000000000000000	0.000000000000000
	Corresponding convergence rates		
3	2.00252	2.00252	2.00250
4	1.99755	1.99469	1.98655

Table 4.5 and Table 4.6 show that **Scheme 0**, **Scheme 1** and **Scheme 2** were able to match the exact solution of Example 3 by at least 14 decimal places. **Scheme 0**, **Scheme 1** and **Scheme 2** took 7, 11 and 21 iterations respectively to converge to the mentioned level of accuracy. The convergence rate of **Scheme 0**, **Scheme 1** and **Scheme 2** is consistently 1 at the various iterations. Varying the value of b does not change the convergence rate of the higher order iterative schemes. The QLM took only 4 iterations to converge to within the 14 decimal digits accuracy. The results show that the QLM converges quadratically as proven in [64, 65].

Table 4.7 presents the infinity norms of the solution $y(x)$ for Example 3 for different number of iterations and varying number of grid points N. The results shown are for each higher order iterative scheme.

Table 4.7: The infinity norms for the approximate solution of $y(x)$ for Example 3 by **Scheme 0, 1, 2** corresponding to varying number of iterations and different number of collocation points(N).

iter.	$N = 50$	$N = 100$	$N = 200$
	Scheme 0		
20	4.950×10^{-16}	4.950×10^{-16}	4.950×10^{-16}
40	1.236×10^{-29}	8.889×10^{-31}	8.889×10^{-31}
60	1.149×10^{-29}	1.596×10^{-45}	1.596×10^{-45}
80	1.149×10^{-29}	3.329×10^{-59}	2.866×10^{-60}
100	1.149×10^{-29}	3.049×10^{-59}	5.146×10^{-75}
	Scheme 1		
20	1.236×10^{-29}	8.889×10^{-31}	8.889×10^{-31}
40	1.149×10^{-29}	3.329×10^{-59}	2.866×10^{-60}
60	1.149×10^{-29}	3.049×10^{-59}	9.241×10^{-90}
80	1.149×10^{-29}	3.049×10^{-59}	1.490×10^{-118}
100	1.149×10^{-29}	3.049×10^{-59}	1.199×10^{-118}
	Scheme 2		
20	1.149×10^{-29}	1.841×10^{-45}	1.841×10^{-45}
40	1.149×10^{-29}	3.049×10^{-59}	1.066×10^{-89}
60	1.149×10^{-29}	3.049×10^{-59}	1.199×10^{-118}
80	1.149×10^{-29}	3.049×10^{-59}	1.199×10^{-118}
100	1.149×10^{-29}	3.049×10^{-59}	1.199×10^{-118}

For each value of N, increasing the number of iterations increases the accuracy of the solution. However, there exists an optimal number iterations such that further increase in the number of iterations does not yield a better solution in terms of accuracy. This is true for all the iterative schemes. For example, in **Scheme 2**, when $N = 200$ increasing the number the number of iterations from 20 to 80 reduces the error in the solution from 8.889×10^{-31} to 1.490×10^{-118}. However, increasing the number of iterations beyond 80 does not improve the accuracy of the solution since the infinity norm for 100 iterations remains at 1.490×10^{-118}. The same can be said about increasing N for each number of iterations. The relationship holds for each iterative scheme.

Chapter 5

Conclusion

In this work, we compared the performance of two spectral hybrid methods namely the spectral relaxation method (SRM) and the spectral local linearisation method (SLLM). Both methods were employed to compute the approximate solution of a coupled system of highly non linear singular BVP modelling the exothermic mass and heat balance in a porous spherical catalytic pellet reacting inside a tubular medium in the presence of mass and heat transfer resistance. Such a problem has an extensive application in biochemical engineering. The validity of the obtained approximate solutions by both methods was verified by the Numerical results and theory. Both the SRM and the SLLM results proved to be valid when compared with theory found in literature. Furthermore, the approximate solutions by both methods are highly accurate when compared against `bvp4c` with a maximum absolute error of 10^{-14}. Both methods converge linearly to the correct solution. However, the SLLM iterative scheme has proven to be much faster than the SRM in terms of the number of iterations it took to converge to the solution of the problem. The SLLM iterative scheme used lesser number of iterations than the SRM.

Furthermore, we presented a novel spectral hybrid method called the spectral Adomian decomposition method abbreviated SADM as a reliable alternative for solving highly non linear BVPs. This method is developed by blending the well known Adomian decomposition method (ADM) with the psuedo spectral collocation method. We further presented a simple modification of the SADM called MSADM which accelerates convergence rate of the SADM by more than twice. The SADM, MSADM and ADM numerical schemes were used to obtain solutions for the popular MDH Jeffery-Hamel flow model and Darcy-Brinkman-Forchheimer momentum equations arising in fluid mechanics. The approximate numerical solutions to the models were compared against exact solution and `bvp4c` where applicable to show that the results were valid. The study revealed that the SADM and MSADM are more robust than the ADM since they produce accurate results for a wider range of governing physical constants that could not be captured by the ADM. This makes the ADM not reliable since it diverges for some governing constants. The MSADM and SADM proved to be exceptionally faster than the ADM since the gap between their computation times was too wide with the ADM being slower. Lastly, the MSADM and SADM demonstrated an extremely higher and acceptable level of accuracy for non linear BVPs.

We discussed another new generalised Reduced quasi linearisation method (RQLM) and its SADM based higher order iteration schemes for finding the solution of a certain class of singular second order two point boundary value problems. This class of BVPs are essential for the study of tumor growth in physiology. The RQLM and its higher order iterative schemes were tested on two physical problem models. These models are thermal distribution in the human head and oxygen diffusion in spherical cells. The method was also tested on a singular second order BVP with an exact solution. The obtained

approximate solutions to each problem by the RQLM and its higher order schemes are validated against `bvp4c`, literature results and exact solution where applicable. The RQLM and its higher order schemes consistently yielded highly accurate results through out the solution space when compared with the QLM. The SADM based higher order iterative schemes (**Scheme 1** and **Scheme 2**) were developed for the RQLM to improve its performance to that of the rapidly converging QLM. For each higher order scheme, the successive higher order scheme took almost half the number of iterations taken by the previous scheme. The convergence rate of the SADM based higher order RQLM is 1. In terms of computation time, the SADM based higher order RQLM schemes (**Scheme 1** and **Scheme 2**) are faster than the QLM.

Bibliography

[1] S. S. Motsa, P. Sibanda, F. G. Awad, S. Shateyi, A new spectral-homotopy analysis method for the MHD JefferyHamel problem, *Computers and Fluids*, 39 1219-1225 (2010).

[2] S. S. Motsa, A new algorithm for solving nonlinear boundary value problems arising in heat transfer, *International Journal of Modeling, Simulation, and Scientific Computing*, 2(3) 355-373 (2011).

[3] S. S. Motsa, P. Sibanda, S. Shateyi, On a new quasi-linearization method for systems of nonlinear boundary value problems, *Mathematical Methods in the Applied Sciences*, 34(11) 1406-1413 (2011).

[4] S. S. Motsa, A new spectral relaxation method for similarity variable nonlinear boundary layer flow systems, *Chemical Engineering Communications*, 201(2) 241-256 (2014).

[5] S. S. Motsa, Z. G. Makukula, On spectral relaxation method approach for steady von Krmn flow of a Reiner-Rivlin fluid with Joule heating, viscous dissipation and suction/injection, *Cent. Eur. J. Phys.*, 11(3) 363-374 (2013).

[6] S. S. Motsa, P. G. Dlamini, M. Khumalo, Solving Hyperchaotic Systems Using the Spectral Relaxation Method, *Abstract and Applied Analysis*, 2012 18 pages (2012).

[7] S.S. Motsa, P. Dlamini, M. Khumalo, A new multistage spectral relaxation method for solving chaotic initial value systems, *Nonlinear Dyn*, 72 265-283 (2013).

[8] S. Shateyi, G. T.Marewo, A New Numerical Approach of MHD Flow with Heat and Mass Transfer for the UCM Fluid over a Stretching Surface in the Presence of Thermal Radiation, *Mathematical Problems in Engineering*, 2013 8 pages (2013).

[9] S. S. Motsa, A New Spectral Local Linearization Method for Nonlinear Boundary Layer Flow Problems, *Journal of Applied Mathematics*, 2013 15 pages (2012).

[10] S. S. Motsa, Z. G. Makukula, S. Shateyi, Spectral Local Linearisation Approach for Natural Convection Boundary Layer Flow, *Mathematical Problems in Engineering*, 2013 7 pages (2013).

[11] S.S. Motsa, P. Sibanda, S. Shateyi, A new spectral-homotopy analysis method for solving a nonlinear second order BVP, *Commun Nonlinear Sci Numer Simulat*, 15 2293-2302 (2010).

[12] D. A. Frank Kamenetskii, Diffusion and heat transfer in chemical kinetics. Plenum Press, New York, (1969).

[13] D. N. Kim, Y. G. Kim, An experimental study of multiple steady states in a porous catalyst due to phase transition, *J. Chem. Eng. Jpn.*, 14 311-317 (1981).

[14] D. N. Kim, Y. G. Kim, Simulation of multiple steady states in a porous catalyst due to phase transition, *J. Chem. Eng. Jpn.*, 14 318-322 (1981).

[15] P. B. Weisz, J. S. Hicks, The behavior of porous catalyst particles in view of internal mass and heat diffusion effects, *Chem. Eng. Sci.*, 17 265-275 (1962).

[16] S. E. H. Elnashaie, F. Uhlig, C. Affane, Numerical Techniques for Chemical and Biological Engineers Using MATLAB, *Springer Science + Business Media*, New York, 2007.

[17] G. Damkohler, Ubertemperatur in kontaktkornern. (Excess temperature in catalyst grains.), *Z. Phys. Chem.*, A193 16-28 (1943).

[18] G. Eigenberger, Institut flir Chemische Verfahrenstechnik, (1992), available at
http://elib.uni-stuttgart.de/opus/volltexte/2009/4798/pdf/eig16.pdf.

[19] O. D. Makinde, Exothermic explosions in a Slab: A case study of series summation technique. *International Communications in Heat and Mass Transfer*, 31(8) 1227-1231 (2004).

[20] D. N. Jaguste, S.K. Bhatia, Partial internal wetting of catalyst particles: hysteresis effects, *AIChE J.*, 37 650-660 (1991).

[21] O. D. Makinde, Strong Exothermic explosions in a cylindrical pipe: A case study of series summation technique, *Mechanics Research Communications*, 32 191-195 (2005).

[22] S. S. Motsa, P. Sibanda, G. T. Marewo, On a new analytical method for flow between two inclined walls, *Numerical Algorithms*, 61(3) 499-514 (2012).

[23] G. B. Jeffery, The two-dimensional steady motion of a viscous fluid, *Phi l. Mag.*, 6 455-465 (1915).

[24] G. Hamel, Spiralformige Bewgungen zaher Flussigkeiten, *Jahresber. Deutsch. Math. Verein.*, 25, 34-60 (1916).

[25] M. G. Bandpay , M. Famouri, F. G. Baboli, Numerical Investigation of Flow through Convergent or Divergent Channel with Finite Difference Method, *GMSARN International Conference on Sustainable Development: Challenges and Opportunities for GMS*, 12-14 (2007).

[26] M. Asadullah, U. Khan, N. Ahmed, R. Manzoor, S. Mohyud-Din, MHD Flow of a Jeffery Fluid in Converging and Diverging Channels, *International Journal of Modern Mathematical Sciences*, 6(2) 92-106 (2013).

[27] D. D. Ganji, M. Azimi, Application of DTM on the MDH Jeffery Hamel problem with nanoparticle, *U.P.B. Sci. Bull.*, 75(1) (2013).

[28] T. A. Nofal, An Approximation of the Analytical Solution of the Jeffery-Hamel Flow by Homotopy Analysis Method, *Applied Mathematical Sciences*, 5(53) 2603-2615 (2011).

[29] A. A. Imani, Y. Rostamian, D. D. Ganji, H. B. Rokni, Analytical Investigation of Jeffery-Hamel Flow with High Magnetic Field and Nano Particle by RVIM, *International Journal of Engineering*, 25(3) 249-256 (2012).

[30] Z. Z. Ganji, D. D. Ganji, M. Esmaeilpour, Study on nonlinear Jeffery-Hamel flow by He's semi-analytical methods and comparison with numerical results, *Computers and Mathematics with Applications*, 58 2107-2116 (2009).

[31] Md. S. Alam, M. A. H. Khan, M. M. Rahman, Critical analysis of the influence of magnetic Reynolds number on MDH Jeffery Hamel Flows, *International Journal of Applied Mathematics and Mechanics*, 9 31-46 (2013).

[32] D. D. Ganji, M. Sheikholeslamia, H. R. Ashorynejad, Analytical approximate solution of Jeffery-Hamel flow with high magnetic field using Adomian Decomposition Method, *ISRN Mathematical Analysis*, 2011 16 pages (2011).

[33] M. Asadullah, U. Khan, N. Ahmed, R. Manzoor, S. T. M. Din, MHD Flow of a Jeffery Fluid in Converging and Diverging Channels, *International Journal of Modern Mathematical Sciences*, 6(2) 92-106 (2013).

[34] Q. Esmaili, A. Ramiar, E. Alizadeh, D.D. Ganji, An approximation of the analytical solution of the JefferyHamel flow by decomposition method, *Physics Letters A*, 372 3434-3439 (2008).

[35] M. Sheikholeslami, D. D. Ganji, H. R. Ashorynejad, H. B. Rokni, Analytical investigation of Jeffery-Hamel flow with high magnetic field and nanoparticle by Adomian decomposition method, *Appl. Math. Mech. -Engl. Ed.*, 33(1) 25-36 (2012).

[36] G. Adomian, L. H. Sibul, R. Rach, Coupled Nonlinear Stochastic Differential Equations, *Journal of Mathematical Analysis and Application*, 92 427-434 (1983).

[37] G. Adomian, A Review of the Decomposition Method in Applied Mathematics, *Journal of Mathematical Analysis and Application*, 135 501-544 (1988).

[38] G. Adomian, L. H. Sibul, Symmetrized solutions for nonlinear stochastic differential equations, *Internal. J. Math. Math. Sci*, 4(3) 529-542 (1981).

[39] H. Jafari, V. D. Gejji, Revised Adomian decomposition method for solving a system of nonlinear equations, *Applied Mathematics and Computation*, 175 1-7 (2006).

[40] A. M. Wazwaz, Adomian decomposition method for a reliable treatment of the Bratu-type equations, *Applied Mathematics and Computation*, 166 652-663 (2005).

[41] A. M. Wazwaz, Adomian decomposition method for a reliable treatment of the EmdenFowler equation, *Applied Mathematics and Computation*, 161 543-560 (2005).

[42] A. M. Wazwaz, A reliable study for extensions of the Bratu problem with boundary conditions, *Mathematical Methods in the Applied Sciences*, 35(7) 845-856 (2012).

[43] A. M. Wazwaz, Pade approximants and Adomian decomposition method for solving the FlierlPetviashivili equation and its variants, *Applied Mathematics and Computation*, 182 1812-1818 (2006).

[44] P. Pue-on, N. Viriyapong, Modified Adomian Decomposition Method for Solving Particular Third-Order Ordinary Differential Equations, *Applied Mathematical Sciences*, 6(30) 1463-1469 (2012).

[45] N. Singh, M. Kumar, Adomian Decomposition Method for Solving Higher Order Boundary Value Problems, *Mathematical Theory and Modeling*, 2(1) 11-22 (2011).

[46] A. K. Singh, G. R. Thorpe, Natural convection in a confined fluid overlying a porous layer - A comparison study of different models, *Indian J. pure appl. Math*, 26(1) 81-95 (1995).

[47] T. A. Abassy, New Treatment of Adomian Decomposition Method with Compaction Equations, *Studies in Nonlinear Sciences*, 1(2) 41-49 (2010).

[48] N. T. Shawagfeh, Nonperturbative approximate solution for Lane-Emden equation, *Journal of Mathematical Physics*, 34(9) 4364-4369 (1993).

[49] M. Alabdullatif, H. A. Abdusalam, E.S. Fahmy, Adomian decomposition method for nonlinear reaction diffusion system of Lotka-Volterra type, *International Mathematical Forum*, 2(2) 87-96 (2007).

[50] A. M. Wazwaz, A new method for solving singular initial value problems in the second-order ordinary differential equations, *Applied Mathematics and Computation*, 128 45-57 (2002).

[51] A. M. Wazwaz, A note on using the Adomian decomposition method for solving boundary value problems, *Foundation of Physics Letters*, 13(5) 493-498 (2000).

[52] I. Mustafa, Decomposition method for solving parabolic equations in finite domains, *Journal of Zhejiang University Science*, 6A(10) 1058-1064 (2005).

[53] R. Montazeri, A Concrete Application of Adomian Decomposition Method, *Int. J. Contemp. Math. Sciences*, 7(24) 1185-1192 (2012).

[54] L. Bougoffa, S. Bougouffa, Adomian method for solving some coupled systems of two equations, *Applied Mathematics and Computation*, 177 553-560 (2006).

[55] A. M. Wazwaz, A reliable modification of Adomian decomposition method, *Applied Mathematics and Computation*, 102 77-86 (1999).

[56] A. R. Vahidi, M. Hasanzade, Restarted Adomians Decomposition Method for the Bratu-Type Problem, *Applied Mathematical Sciences*, 6(10) 479-486 (2012).

[57] D. J. Evans, K. R. Raslan, The Adomian decomposition method for Solving delay differential equation, *International Journal of Computer Mathematics*, 82(1) 49-54 (2005).

[58] M. H. Hamdan, Single-phase flow through porous channels: A review. Flow models and channel entry conditions, *Journal of Applied Mathematics and Computations*, 62(2) 203-222 (1994).

[59] M. M. Awartani, M. H. Hamdan, Fully developed flow through a porous channel bounded by flat plates, *Applied Mathematics and Computation* 169 749-757 (2005).

[60] K. Hooman, A perturbation solution for forced convection in a porous saturated duct, *Journal of Computational and Applied Mathematics*, 211 57-66 (2008).

[61] J. A. Adam, A simplified mathematical model of tumor growth, *Mathematical Biosciences*, 81(2) 224-229 (1986).

[62] J.A. Adam, A simplified mathematical model of tumor growth II: effect of geometry and spatial nonuniformity on stability, *Mathematical Biosciences*, 86(2) 183-211 (1987).

[63] R. Bellman and R. Kalaba, Quasilinearization and Nonlinear Boundary Value Problems, *Amer. Elseiver*, New York, (1965).

[64] V. B. Mandelzweig, Quasilinearization method and its verification on exactly solvable models in quantum mechanics, *J. Math. Phys.* 40(12) 6266-6291 (1999).

[65] V. B. Mandelzweig, Quasilinearization method, Nonperturbative approach to physical problems,*Physics of Atomic Nuclei*, 68(7) 1227-1258 (2005).

[66] B. Ahmad, J. J. Nieto, N. Shahzad, The Bellman-Kalaba-Lakshmikantham Quasilinearisation method for Neumann problems, *Journal of Mathematical Analysis and Applications*, 257 356-363 (2001).

[67] R. S. N. Alsaedi, Generalized Quasilinearization Method for the Forced Duffing Equation with Mixed B.C., *International Mathematical Forum*, 1(40) 1975-1982 (2006).

[68] J. J. Nieto, Generalized Quasilinearization method for a second order ordinary differential equation with dirichlet boundary conditions, *American mthematical society*, 125(9) 2599-2604 (1997).

[69] W. F. Ford, J. A. Pennline, Singular non-linear two-point boundary value problem: Existence and Uniqueness, *Nonlinear Analysis*, 71 1059-1072 (2009).

[70] S.S. Motsa, P. Sibanda, A linearisation method for non-linear singular boundary value problems, *Computers and Mathematics with Applications*, 63 1197-1203 (2012).

[71] H. Çaglar, N. Çaglar, M. zer, B-spline solution of non-linear singular boundary value problems arising in physiology, *Chaos Solitions and Fractals*, 39 1232-1237 (2009).

[72] R. K. Pandey, A. K. Singh, On the convergence of a finite difference method for a class of singular boundary value problems arising in physiology, *J. Comput. Appl. Math*, 166 553-564 (2004).

[73] M. Abukhaled, S. A. Khuri, A. Sayfy, A numerical approach for solving a class of singular boundary value problems arising in physiology, *International Journal of Numerical Analysis and Modeling*, 8 353-363 (2011).

[74] J. Rashidinia, R. Mohammadi, R. Jalilian, The numerical solution of non-linear singular boundary value problems arising in physiology, *Applied Mathematics and Computation*, 185 360-367 (2007).

[75] S. A. Khuri, A. Sayfy, A novel approach for the solution of a class of singular boundary value problems arising in physiology, *Mathematical and Computer Modelling*, 52 626-636 (2010).

[76] O. D. Makinde, Non-perturbative solutions of a nonlinear heat conduction of the human head, *Scientific Research and Essays*, 5(6) 529-532 (2010).

[77] L. N. Trefethen, Spectral Methods in MATLAB, SIAM, Philadelphia, USA, 2000.

[78] L. N. Trefethen, Finite difference and spectral methods for ordinary and partial differential equations, Upson Hall, New York, USA, 1996.

[79] G. Adomian, A review of the decomposition method and some recent results for nonlinear equation, *Math. Comput. Modelling*, 13(7) 17-43 (1990).

[80] G. Adomian, R. Rach, Noise terms in decomposition series solution, *Comput. Math. Appl.*, 24(11) 61-64 (1992).

[81] G. Adomian, Solving frontier problems of physics: The decomposition method, Kluwer, Boston, MA, (1994).

[82] A. M. Wazwaz, A new algorithm for solving singular initial value problems in the second-order differential equations *Appl. Math. Comput.*, 128 45-57 (2002).

[83] A. M. Wazwaz, Adomian decomposition method for a reliable treatment of the Emden-Fowler equation, *Appl. Math. Comput.*, 161 543-560 (2005).

[84] S. Abbasbandy, E. Shivanian, Exact analytical solution of the MDH Jeffery-Hamel flow problem, *Mecannica*, 47 1379-1389 (2012).

[85] S. S. Motsa, P. Sibanda, F.G. Awad, S. Shateyi, A new spectral-homotopy analysis method for the MHD JefferyHamel problem, *Computers and Fluids*, 39 1219-1225 (2010).

[86] H. S. Lin, Oxygen diffusion in a spherical cell with nonlinear oxygen uptake kinetics, *J Theor Biol*, 60 449-57 (1976).

[87] P. Hiltmann, P. Lory, On oxygen diffusion in a spherical cell with MichaelisMenten oxygen uptake kinetics, *Bulletin of Mathematical Biology*, 45(5) 661-664 (1983).

[88] S. S. Motsa, P. Sibanda, Some modifications of the quasilinearization method with higher-order convergence for solving nonlinear BVPs, *Numer Algor*, 63 399-417 (2013).